84 P

NASA CR-54054
TRW ER-5847

N64-22453
CODE-1 CAT. 27

# SUMMARY REPORT ON

# TRANSVERSE FIELD ION ENGINE DEVELOPMENT

OTS PRICE
XEROX $ 8.10 ph
MICROFILM $ none


By
W. N. Huss and A. C. Eckert


Prepared for
NATIONAL AERONAUTICS AND SPACE ADMINISTRATION
CONTRACT NAS8-2527


TRW ELECTROMECHANICAL DIVISION
THOMPSON RAMO WOOLDRIDGE INC.
CLEVELAND, OHIO

## NOTICE

This report was prepared as an account of Government sponsored work. Neither the United States, nor the National Aeronautics and Space Administration (NASA), nor any person acting on behalf of NASA:

A.) Makes any warranty or representation, expressed or implied, with respect to the accuracy, completeness, or usefulness of the information contained in this report, or that the use of any information, apparatus, method, or process disclosed in this report may not infringe privately owned rights; or

B.) Assumes any liabilities with respect to the use of, or for damages resulting from the use of any information, apparatus, method or process disclosed in this report.

As used above, "person acting on behalf of NASA" includes any employee or contractor of NASA, or employee of such contractor, to the extent that such employee or contractor of NASA, or employee or such contractor prepares, disseminates, or provides access to, any information pursuant to his employment or contract with NASA, or his employment with such contractor.

Request for copies of this report should be referred to

National Aeronautics and Space Administration
Office of Scientific and Technical Information
Attention: AFSS-A
Washington, D. C. 20546

CASE FILE COPY

193786

NASA CR-54054
TRW ER-5847

FINAL REPORT

# SUMMARY REPORT ON TRANSVERSE FIELD ION ENGINE DEVELOPMENT

by

W. N. Huss and A. C. Eckert

prepared for

NATIONAL AERONAUTICS AND SPACE ADMINISTRATION

March 1964

CONTRACT NAS8-2527

Project Manager
NASA Lewis Research Center
Cleveland, Ohio
Spacecraft Technology Division
James A. Wolters

TRW ELECTROMECHANICAL DIVISION
Thompson Ramo Wooldridge Inc.
23555 Euclid Avenue
Cleveland, Ohio 44117

## ABSTRACT

A gaseous discharge possessing good ion-focusing properties has been investigated and applied to the design of an ion source for electrical propulsion. The discharge takes place in the presence of a shaped magnetic field, which establishes the potential distribution necessary for focusing ions on the exit aperture of the source. Electrons are introduced into the discharge and migrate across the magnetic field by collision processes until they are removed at an anode. Electron mean free paths are long compared to the discharge chamber dimension. As a consequence, motion along magnetic field lines is relatively unconstrained within the discharge, permitting the development of uniform charge densities over surfaces of constant magnetic field strength. The resultant potential distribution possesses equipotential surfaces that are closely coincident with the surfaces of constant magnetic field strength. With suitably simple geometries, this means of controlling the potential distribution permits the removal through the exit aperture of virtually all the ions formed.

An ion source employing the above concepts has been fabricated and has undergone initial performance evaluation tests with both argon and mercury propellants. The performance evaluation program was oriented toward determining the feasibility of utilizing the source in a space propulsion application. The operation characteristics of the source were investigated and modifications to improve the performance were made throughout the program. A significant parameter modification was made when the magnetic pole piece included angle was increased. It was determined that the magnetic field distribution within the ion source could be tailored to obtain a more efficient discharge by increasing the magnetic pole piece included angle. The performance level of the ion source became very good when the magnetic pole piece included angle was increased to $5\pi/6$. Probe measurements of the plasma within the source were made and the results were consistent with the theoretical expectations. The probe measurements of the arc plasma gave data relative to the energy distribution of the high energy electron group in the plasma. Plasma potential distribution data was also obtained from the probe measurements.

Tests of ion source performance with a mercury propellant were made. Arc efficiency has been obtained at a level of 200 eV/ion in the 95 to 100 per cent propellant utilization region with tungsten cathodes. The ion beam density at these performance levels was about 50 $ma/cm^2$ at the exit aperture. The performance data was obtained with an ion source that used an accel-decel extraction system. Major efforts have been made on the problems of ion source efficiency, ion acceleration, and nickel matrix dispenser cathodes. The transverse field ion source appears attractive in the space propulsion application due to its excellent efficiency, high propellant utilization, and good lifetime potential.

TABLE OF CONTENTS


| | Page |
|---|---|
| Abstract | i |
| Table of Contents | ii |
| List of Figures | iii |
| List of Pictorials | iv |
| List of Tables | v |
| List of Symbols | vi |
| 1.0 INTRODUCTION | 1 |
| 2.0 TECHNICAL DESCRIPTION OF PROGRAM | 7 |
| 2.1 Transverse Field Ion Source Research Program | 13 |
| 2.1.1 Source Optimization | 17 |
| 2.1.2 Seven-Inch Diameter Ion Source (Argon Propellant) | 24 |
| 2.1.3 Diagnostics for Argon Propellant | 24 |
| 2.1.4 Seven-Inch Diameter Ion Source (Mercury Propellant) | 34 |
| 2.2 Extraction Electrode Studies | 39 |
| 2.2.1 Four-Inch Diameter Ion Source (Mercury Propellant) | 51 |
| 2.2.2 Two-Inch Diameter Ion Source (Mercury Propellant) | 58 |
| 2.3 Cathode Studies | 63 |
| 3.0 SUMMARY AND CONCLUSIONS | 74 |
| 4.0 REFERENCES | 75 |

## LIST OF FIGURES


| Figure No. | Title | Page |
|---|---|---|
| 1.0.1 | Transverse Field Ion Source Concept | 2 |
| 2.1.1 | Initial Research Model Configuration (Cross Section View) | 15 |
| 2.1.2 | Field Dependence on Pole Face Angle | 22 |
| 2.1.3 | Performance Characteristics of Initial Research Model | 23 |
| 2.1.4 | The Enlarged Arc Chamber Detail (Cross Section View) | 25 |
| 2.1.5 | Performance Characteristics of the Transverse Field Ion Source with the Enlarged Arc Chamber | 26 |
| 2.1.6 | Typical Probe Characteristic Curve | 28 |
| 2.1.7 | Probe Construction Cross Section | 29 |
| 2.1.8 | Probe Electrical Circuit | 33 |
| 2.1.9 | Electron Energy Distribution | 35 |
| 2.1.10 | Performance Characteristics with a Mercury Propellant | 37 |
| 2.2.1 | Resonant Charge Exchange Cross Sections Versus Ion Velocity | 43 |
| 2.2.2 | Movable Extraction System Detail | 46 |
| 2.2.3 | Geometry of Extraction System | 48 |
| 2.2.4 | Initial Acceleration Electrode Interception Data | 49 |
| 2.2.5 | Variable Acceleration Distance Electrode Interception Performance Data | 50 |
| 2.2.6 | Four-Inch Diameter Transverse Field Ion Source | 52 |
| 2.2.7 | Inner Acceleration Electrode Mounting Arrangement | 61 |
| 2.3.1 | Cathode Assembly Detail I | 64 |
| 2.3.2 | Cathode Assembly Detail II | 66 |
| 2.3.3 | Performance Characteristics of the Two-Inch Ion Engine with a Powdered Nickel Matrix Cathode | 68 |
| 2.3.4 | Cathode Assembly Detail III | 70 |
| 2.3.5 | Cathode Assembly Detail IV | 71 |

## LIST OF PICTORIALS


| Pictorial No. | Title | Page |
|---|---|---|
| 2.1.1 | Initial Research Test Model | 16 |
| 2.1.2 | Initial Research Facility | 18 |
| 2.1.3 | Calorimeter Erosion Detail | 20 |
| 2.1.4 | Probe Detail | 30 |
| 2.1.5 | Probe Linkage | 31 |
| 2.1.6 | Diagnostic Test Model | 32 |
| 2.2.1 | Four-Inch Ion Engine (3/4 View) | 53 |
| 2.2.2 | Four-Inch Ion Engine (Top View) | 54 |
| 2.2.3 | Four-Inch Ion Engine (Front View) | 55 |
| 2.2.4 | Experimental Facility | 56 |
| 2.2.5 | Two-Inch Ion Engine (3/4 View) | 60 |

## LIST OF TABLES


| Table No. | Title | Page |
|---|---|---|
| 2.0.1 | Ionization Loss | 10 |
| 2.2.1 | Ion Engine Efficiency as a Function of Various Propellants | 41 |
| 2.2.2 | Performance Data of Four-Inch Diameter Ion Engine | 57 |
| 2.2.3 | Performance Data of Two-Inch Diameter Ion Engine (Tungsten Cathode) | 62 |
| 2.3.1 | Performance Data of Two-Inch Diameter Ion Engine with Nickel Matrix Cathode (Powdered) | 67 |

## LIST OF SYMBOLS

| | | |
|---|---|---|
| $e$ | - | electronic charge |
| $E_A$ | - | average electron energy in plasma |
| $j$ | - | ion current density |
| $K_o$ | - | correction factor |
| $m$ | - | mass of ion |
| $M$ | - | mass of mercury atom |
| $N_+$ | - | ion density of plasma |
| $v$ | - | velocity |
| $V_a$ | - | acceleration voltage |
| $X$ | - | position at which width of ion beam is Y |
| $X_o$ | - | acceleration distance |
| $Y$ | - | width of ion beam |
| $Y_o$ | - | initial width of ion beam |
| $\eta$ | - | power efficiency |

## 1.0 INTRODUCTION

One problem common to all existing bombardment ion sources for propulsive use is that of ion collection. In all current designs, only a small fraction of the ions produced are collected and removed through the source exit apertures. The remainder recombine inside the sources, giving up energy to the bombardment chamber walls.

Notwithstanding this seemingly excessive loss of ions, bombardment sources have shown themselves capable of power efficiencies substantially higher than have been obtained by competing types.[1,2] However, it is clear that the way is open to significant increases in both efficiency and range of application of ion engines through improvements in the collection and utilization of the ions produced. The concept of the ion source to be described here grew out of an effort to solve this collection problem for a source suitable for propulsive purposes.

The basis of the collection problem in current designs may be stated simply as follows. All these designs have electron mean free paths with lengths of at least the order of bombardment chamber dimensions. In order to utilize the energy of the electrons to create ions rather than dissipating it on electrodes, some sort of electron trapping mechanism is used. These mechanisms prevent electrons from reaching the discharge anode until they have undergone several collisions with gas atoms. This technique has been successful in producing copious ion supplies in several different source designs. The resultant plasmas that form in the trap region are not neutral, however, for the same electric fields that hold the negative electrons in the traps are equally effective in expelling the positive ions from the traps. The net result is a forceable outstreaming of ions from the trap region. In the more elementary source designs, this outstreaming is largely uncontrolled and virtually all the ions produced recombine internally at some negative electrode surface. Only a few escape through the exit aperture and become available for propulsion. In more advanced designs, the trapping fields are shaped to direct a larger fraction of the ions through the exit apertures. Nonetheless, the best source designs to date require several hundred electron volts input for each ion extracted through the exit aperture. This energy is, of course, far in excess of that theoretically needed to produce an ion.

In the source concept presented here, a deliberate attempt was made to avoid the creation of a trap from which ions would be expelled in more than one direction. Figure 1.0.1 will help to clarify the concept. A pair of magnet poles with a wedge shaped gap are placed as shown. The magnetic field lines in the gap will

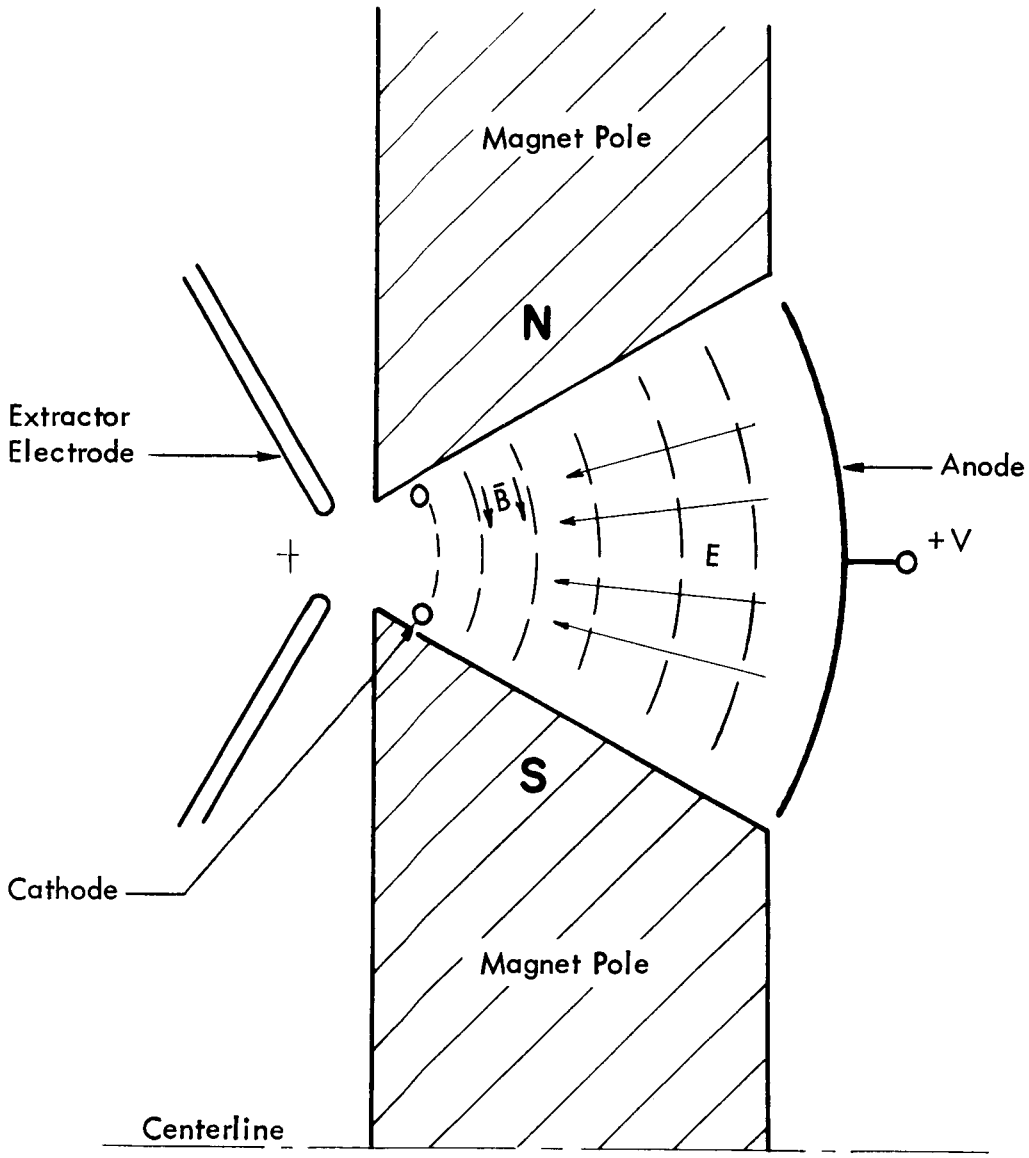


FIGURE 1.0.1 TRANSVERSE FIELD ION SOURCE CONCEPT

approximate sectors of concentric circles and are shown as dashed lines. Cathodes are placed near the narrow end of the gap and held at the magnet pole potential. At the large end of the gap an anode is placed with its inner surface conforming to the shape of the field lines.

Gas is admitted to the chamber and a discharge is obtained between the cathodes and anode. The magnetic field should be sufficiently strong to make the cyclotron radii of the electrons very small compared to the anode-cathode distance. Electron mean free paths are assumed at least equal in length to the anode-cathode distance. Electrons emitted from the cathodes translate freely along the magnetic field lines in spiral paths of small radius. This creates a sheet of electrons across the narrow gap between the pole pieces. Net electron motion toward the anode is prevented by the magnetic field unless the electrons undergo multiple collisions with gas atoms. Under the latter circumstances migration to the anode takes place where the electrons are collected. Some electron energy is lost in the collision processes, of course, but provided a suitable electric field is maintained, the average electron energies can be kept in the neighborhood of 25 eV at all points in the chamber. At these energies in mercury vapor, a reasonable fraction of all inelastic collisions result in ionization, so ion production is seen to proceed in an efficient manner.

A plasma will be created in the chamber with its characteristic sheath forming over all material walls. The free translation of electrons along the magnetic field direction is expected to form unipotential surfaces inside the plasma body which coincide with the shapes shown for the field lines in the figure. The resultant electric field in the plasma body will then be directed perpendicular to these unipotentials as indicated by the arrows. The particular choice of geometry used here approximates cylindrical geometry with the origin shown by the small cross to the left of the narrow gap. Because of the shape of the electric field, ions formed anywhere in the plasma body will be accelerated toward this origin, so that the narrow gap serves as the exit aperture of the source. It should be noted that because of the small charge to mass ratio of the ions, the ionic paths will be negligibly affected by the magnetic field.

The ion loss to the chamber walls through the sheaths has been neglected in this crude description, of course, but elementary theoretical treatments of the problem put this loss at less than ten per cent of the total number of ions formed. Another feature of great importance is the fact that because of the direction of

the electric and magnetic fields, the electrons experience strong forces perpendicular to the plane of the diagram in Figure 1.0.1. Thus in a linear source of this type, the electrons would be all swept to one end of the chamber. The obvious answer to this problem is to form a figure of revolution about the center line shown. The lateral migration of the electrons in this arrangement would simply result in a circulation of electrons about the center line. No interaction of this motion with the ion collection mechanism is expected.

From the description above, it can be seen that an annular ion source can be constructed that holds the promise of extreme efficiency by virtue of good internal ion focusing. The potential application of such a source is obvious, as it could extend the use of ion engines into the low specific impulse range where no suitable electric propulsion device now exists.

Before a practical development of this ion source concept could be undertaken, it was necessary to experimentally establish the operating characteristics of the ion source. The presence of the crossed electric and magnetic fields eliminated the possibility of a simple theoretical treatment of the problem. Approximate operating parameters were established and an initial research test model was constructed and tested. This initial test model proved valuable in subsequent diagnostic work (argon propellant) in establishing the operating parameters and in proving the concept of the discharge.

The practical development of the transverse field ion source was then undertaken with a change from argon to a mercury propellant. A modified version of the initial test model was used and very good performance was obtained with the mercury propellant operation. It became evident at this point that the ultimate in ion source efficiency was being approached. Further research on improving the ion source efficiency was deferred since it became apparent that there was a relationship between the extraction system and the source performance. The location and potential of the extraction system influenced the plasma meniscus and the cathode emission. Thus, it was determined that extraction system development should be initiated and that the research on the extraction system and on further improving the ion source efficiency should proceed concurrently.

The approach taken to the acceleration system sputtering problem was similar to the approach investigated under Contract NAS8-42. The amount of sputtering was to be minimized by proper choice of propellant and by optimizing the geometry in the acceleration region. That sputtering which was unavoidable was to be directed to regions

of the electrodes unimportant from a focusing standpoint. In taking this approach, it was accepted that an accel-decel electrode system would be used, since such a system appears to best satisfy neutralization requirements while permitting the desired control over the relationship between current density and electrode spacing.

Accel-decel systems inherently incur some sputtering damage to the accel electrode, since ions formed by charge exchange below the final electrode and beam potential cannot escape to space or to any other electrode. The intent was to direct the charge exchange ions away from the upstream surfaces of the accel electrode, since these surfaces are important in establishing the current density and contour of the ion beam. All charge exchange ions formed above the final electrode potential were to be expelled into space. On the downstream side of the accel electrode, this occurs inherently. On the upstream side, the approach was to keep primary particle trajectories directed along the accelerating field direction, so that charge exchange ions formed in this region would be focused along with the primary beam, thus missing the accel electrode and passing out into space.

The extraction system research was initiated applying the theoretical concepts to an extraction system design using a modified Pierce geometry. The approach was to demonstrate experimentally a flat or concave meniscus at the source extraction aperture and then to experimentally optimize the extraction system. The initial testing encountered some problems with corona discharges and insulator breakdowns, but these problems were solved and high voltage operation utilizing an accel-decel extraction system was obtained. It became evident at this time that the modified version of the initial test model was no longer suitable for testing due to power supply difficulties in the extraction of a 500 ma ion beam. The problem was basically overtaxed power supplies. A new four-inch diameter ion source was constructed and then suitable extraction system performance was obtained. At this point in the program, excellent ion source performance had been coupled with an acceptable (for testing purposes) extraction system. Further extraction research was not within the scope of this program.

The remaining major problem area to be solved was to install an efficient nickel matrix dispenser cathode in the ion source. Previously, a tungsten wire cathode had been used. Development of a good nickel matrix cathode arrangement was initiated and it was soon discovered that the magnetic field suppressed electron emission from cathode surfaces oriented parallel to the magnetic field. Correction in the design was made to account for the magnetic field influence and good ion source operation was obtained except that the arc voltage was too high for long cathode life expectancy.

The research was then directed toward improving the electron emission characteristics of the cathode and progress was made in this area. At this point, the contract expiration for the experimental research was reached and the experimental work was terminated.

## 2.0 TECHNICAL DESCRIPTION OF PROGRAM

In the previous section of this report, the basic concept of the transverse field ion source was described. In this section, the considerations behind the various aspects of the design will be dealt with in greater detail, and the potentialities of the ion engine will be indicated. Upon this background, the course of the developmental program will be discussed, covering all work performed under Contract NAS8-2527.

The ionization efficiency of an electron bombardment discharge source is essentially independent of the size, or scale, of the source, provided gas pressure, current densities, etc. are adjusted to the appropriate values for the scale used. The physical processes behind this scale independence are of interest since the extra degree of freedom in design which is allowed by this property constitutes the principal advantage of bombardment sources over contact ionization sources.[2] With arbitrary current densities available at constant efficiency, the current density commensurate with the required electrode life for any application can always be obtained with no penalty from either power or propellant efficiency standpoints. This additional degree of freedom gives the needed flexibility in design, allowing bombardment engines to be constructed on the basis of lifetime alone, provided that sizes and weights are maintained at reasonable levels.

The processes which an electron undergoes in a bombardment engine are basically three types of encounters with gas atoms. The electrons may undergo elastic collisions, they may undergo inelastic collisions which result in excited gas atoms, or they may ionize the gas atoms. For the ionization event to occur, the electrons must enter the ionizing region with energies in excess of the ionization potential of the gas atoms. At energies of this magnitude, the energy loss of the electrons in elastic collisions is negligible compared to the inelastic processes. For all practical purposes, the energy transfer all goes into the ionization and excitation of atoms.

The relative amounts of ionization and excitation depend upon the ratios of the cross sections for these two processes. These cross sections are strongly dependent upon electron energy in the region below one hundred volts. Below the ionization threshold, none of the energy goes into ionization; however, as the electron energy increases, an increasing fraction of the energy goes into ionization. At two or three times the ionization threshold, comparable amounts of energy are usually expended in ionization and excitation, with the exact division depending

on the propellant material used. As electron energies are increased still higher, the ratio of ionization to excitation generally shows a slow increase, reaches an asymptotic value in the low KeV range, and then remains essentially constant up to particle energies in the MeV range.

This behavior is well known[3] and is utilized in many types of particle detectors for nuclear physics experiments in which particle energies are measured in terms of the ionization they produce. In the region of constant energy sharing, it is customary to speak of the total amount of energy dissipated in the production of each ion-electron pair. This quantity is about 30 electron volts for most materials. It varies only a few electron volts in either direction from this figure for most elements, being lowest for the noble gases and highest for the alkali metals.

From the above description, it is clear that the bombardment ionization process itself is scale independent. The fraction of electron energy going into ionization is seen to be strictly a matter of competition between the ionization and excitation processes. The cross section ratios which determine this fraction are characteristic of the propellant material used and the energy of the bombarding electrons. Neither of these depends on engine size, gas density, or any other factor which could be related to scaling.

The matter of scale dependence of other processes which influence ion source efficiency cannot be seen so directly, since they depend not only on fundamental physical processes, but on additional conditions necessary for the operation of an ion engine. In order to examine these conditions, a workable concept for a bombardment engine shall be developed.

Based on the above value of 30 electron volts per ion, it can be easily shown that the bombardment of propellant atoms by energetic electrons constitutes an ion source concept with an extremely high potential power efficiency. Consider for example, the use of mercury as a propellant in an engine operating at a specific impulse of 5,000 seconds. The energy expended accelerating a mercury ion to the velocity corresponding to 5,000 seconds specific impulse is 2,500 electron volts. If each ion required only 30 electron volts for its production, the power efficiency of the engine would be

$$\eta = \frac{\text{Acceleration energy}}{\text{Production energy + Acceleration energy}}$$

$$\eta = \frac{2500}{30 + 2500} = 99 \text{ per cent}$$

The above idealization does not include any of the inefficiencies or compromises necessary in achieving a practical ion engine. The development of a workable concept is not so simple. First, there is the matter of collecting the ions formed and sweeping them out of the ionization region into a region from which they may be accelerated to provide reaction thrust. Good collection efficiency requires that the ion mean free paths be large compared with the ionization region depth (in the direction of sweeping) in order that collisions with neutral atoms will not scatter the ions excessively. This is important, not only from the standpoint of efficient ion collection, but also to prevent loss of neutrals which could be knocked out of the ion source by ion collisions. These considerations fix the maximum neutral density, which is a limiting factor in available ion current density. It appears possible in virtually all cases of interest to keep the ion-neutral interaction negligibly low, so that this factor need not contribute appreciably to any loss in efficiency. The matter of collecting the ions formed thus becomes completely a problem of properly shaping the electric fields within the ionizing region.

The second matter of importance in reducing the idealized engine to a workable device is the requirement of holding the electrons within the ionizing region until their energy is largely dissipated. The electron cross sections for inelastic collisions are usually substantially smaller than the ion-neutral collision cross sections, so that the electron mean path length prior to an inelastic collision will generally be many times the ion mean free path. Since the ion mean free path must be made large compared to the ionizing region depth, it is evident that the electron path length prior to an inelastic collision will be very large compared to this depth. Thus, if electrons were simply injected into the ionizing region with no constraints on their motion, they would quickly escape, having given up only a small fraction of their energies in the form of ionization and excitation.

In order to obtain a large fraction of the electron energy in the form of ionization and excitation of the propellant, it is necessary to form either a magnetic or electric trap which increases the electron path length in the ionizing region to a value at least comparable with the mean path for inelastic collisions. The trap of interest is a crossed electric and magnetic field configuration in which electron motion from the cathode to the anode is constrained magnetically while electron motion in the perpendicular direction at the chamber walls is constrained electrostatically. In this trap, the voltage can reach the value utilized in accelerating the electrons initially, and it is here that we encounter a fundamental, though not serious, restriction on the conditions necessary in a workable ion engine.

Since ions may be formed anywhere within the electron trap, some are capable of achieving energies corresponding to the peak voltages within the ionizing region, and subsequently bombarding the walls of the ionizing chamber at those energies. It is important to keep the ion energies below the sputtering threshold of the chamber material in order to avoid destruction of the walls by ion bombardment. This consideration places an upper limit of about 45 electron volts on the ion energies for the most resistant structural materials, and therefore, limits the electron energies also to about 45 electron volts. If other electrodes at or below the chamber wall potential are exposed to bombardment by ions formed in the trap, they may be the determining elements in fixing the maximum electron energies. For instance, an exposed oxide cathode would impose a limit of about 25 electron volts on ion and electron energies.

At electron energies in the 25 to 45 electron volt range, the division of electron energies between ionization and excitation is generally not quite as favorable as in the high energy region, but nonetheless ions can still be generated at good efficiency. Table 2.0.1 shows the ionization behavior of several materials in both the low and high energy regions. Experimental data for the energy loss for each ion-electron pair formed is shown for electrons shot into a gas at various energies and allowed to completely dissipate their energies in the gas. Here it is seen that mercury is an especially good material from an ionization efficiency standpoint. While most materials show energy requirements of 50 to 60 electron volts per ion formed in the low energy range, mercury is seen to require only about 30. (Ref. 4).

Table 2.0.1

Ionization Loss (eV/ion-electron pair)

| Electron Energy | 30 eV | 50 eV | 75 eV | 100 eV | 200 eV | E ≅ 1 KeV | E > 4 KeV |
|---|---|---|---|---|---|---|---|
| He | | 42 | | 34 | | 31 | |
| $N_2$ | | | 58 | 63 | | 45 | 36 |
| A | 67 | 56 | | 63 | | 33 | 29 |
| Hg | 27 | 36 | | 37 | 38 | | |

From the above, it is seen that sputtering considerations require that bombardment ion sources operate with peak electron energies below about 45 electron volts. The ionization properties of materials as typified in Table 2.0.1 show that this

restriction does not necessarily entail an efficiency penalty in comparison with the idealized ion engine discussed earlier. In fact, the table indicates that by using mercury as the propellant and by injecting ionizing electrons at 30 electron volts, a workable ion engine could in principle have a higher efficiency than the idealized engine. Only 27 electron volts per ion are required at this energy as compared to 30 which was assumed for the idealized engine.

Of the conditions found necessary for a workable engine, the electron energy limitation clearly bears no relationship to engine scaling. The requirement of a magnetic electron trap could lead to a scaling consideration, however, if we were to assume that the trapping field was supplied by an electromagnet. The power required by the electromagnet would detract from the efficiency and scales in such a direction as to favor large engines. However, making the assumption that the field is supplied by permanent magnets removes the dependence completely. Not only do permanent magnets require no power, but they are of constant mass per unit engine thrust, regardless of scale. We will adopt the latter assumption since it yields highest efficiency and since it is always possible in principle to design a suitable permanent magnet circuit of reasonable weight.

One last feature which must be considered with regard to power efficiency is the electron source. It is necessary to operate at low electron energies and this condition virtually requires that we depend on thermionic cathodes to supply the electrons, there being no other convenient low energy electron source. The energy requirement plus the necessity of an effective trap allows us to see the relationship between cathode power and scaling. Let us assume that the electrons are injected at a constant energy consistent with the sputtering consideration discussed above. Provided these electrons are effectively trapped, it is apparent from Table 2.0.1 that each electron injected will produce a given number of ions. Thus, the ions are produced at a given efficiency independent of scale, so that a fixed electron current is required for a given rate of ion generation. Under the mean free path conditions imposed earlier, the rate of ion-electron recombination in the source is negligible, and the ion collection efficiency becomes scale independent, being solely a function of source geometry. Thus, it is seen that the ion current delivered to the accelerating region is proportional to the injected electron current, which implies a fixed cathode size and power for a given thrust, irrespective of engine scale.

From the above discussion, it is seen that all the factors relating to power efficiency are independent of the scale of an ion source of a given design. It was pointed

out, however, that a maximum neutral atom density existed for any given ion chamber depth. The condition which determines the allowable neutral atom density is the requirement that the ions undergo negligible collisions with neutrals in being swept from the ionizing chamber into the accelerating region. Since the collision probability (for values near zero) varies directly with the neutral density, this density should vary inversely with chamber depth to hold the collision probability at a constant value. Thus, it is seen that the neutral density must vary inversely with engine scale for a constant ion collection efficiency.

In order to show the complete independence of bombardment source design from scaling effects, it is necessary to show that the required neutral gas density behavior with engine size is compatible with constant propellant utilization efficiency. The basic principle of operation of a bombardment engine is to allow gas atoms to enter the ionization chamber where they drift at thermal velocities until they are either ionized or drift out the exit port leading to the acceleration region. The neutral-neutral collision cross section is generally of the same order as the neutral-ion collision cross section. Thus, the neutral mean free path is of the same order as the ion mean free path, which was made long compared to the chamber depth. As a result, the neutral atoms can be thought of as undergoing no interactions except with electrons while drifting across the ion chamber. In order to achieve high propellant utilization, the probability of an atom undergoing an ionizing collision during the time required for it to drift across the chamber must be very close to unity. If the probability is much lower than this value, a sizable fraction of the neutrals will drift out of the exit port and be lost.

In order for the probability of ionization to be close to unity, the integrated product of the number of electrons per unit area per unit time which stream past the atom during its traversal of the chamber times their cross section for ionization must be much greater than unity. This integral is numerically equal to the number of ionization lengths per drift path for the atom and is proportional to both the average electron current density and path length. For the propellant utilization to be independent of scale, then, the average electron current density must vary inversely with the linear size of the engine. This condition is not in conflict with any requirement for high power efficiency, so it is seen that both high power efficiency and high propellant efficiency can be obtained simultaneously in any engine size range.

Lumping together the requirements for this achievement of flexibility in size at constant efficiencies quickly yields the variation of other quantities with engine size. The ion current density behavior, for instance, is directly derivable from the neutral atom density, since the rate of ion production is proportional to the number of atoms per unit time drifting into the ionizing region. This number is in turn proportional to the mean thermal velocity of the neutral atoms times their mean density. Since the neutral atom density was required to vary inversely with the size, so must the ion current density.

The total ion current, and thus the engine thrust, is porportional to the ion current density times the exit port area, the latter being proportional to the square of the size. Consequently, the ion current and thrust vary linearly with engine size.

The size dependence of the magnetic trapping field is also easily shown. The function of the trap is to contain the electrons until they have undergone a sufficient number of collisions to insure that the bulk of their energies have been absorbed in inelastic processes. Since the electrons are to be injected at a given energy, a fixed number of collisions are required to accomplish this absorption. With each collision, an electron of given energy can migrate perpendicular to the field some fraction of a Larmor radius on the average, so that the Larmor radius should be a particular fraction of the trap size, for electrons to be contained for a given number of collisions. Thus, the Larmor radius, which is inversely proportional to magnetic field strength, should scale directly with engine size. The magnetic field strength, therefore, varies inversely with size for constant trapping efficiency. Incidentally, the electric fields can be seen to do likewise since they are inversely proportional to electrode spacings for given voltage differences.

## 2.1 Transverse Field Ion Source Research Program

The preceding section described the basis upon which the transverse field ion source concept was developed. The primary aim in the transverse field ion source concept was to provide an efficient means for collecting the ions by properly shaping the electric fields within the ionizing region, as described in the introduction. Upon the theoretical establishment of the concept, the promise of the transverse field ion source was sufficiently great to merit funding of experimental research under NASA Contract NAS8-2527 to establish experimentally the feasibility of this concept.

The initial work was directed toward the theoretical determination of the important parameters of the ion source. The theory of operation for this source is straightforward in its simplest form. If one attempts to refine the theory to treat details such as electrode form and spacing, however, the formalism rapidly gets out of hand. These details are more amenable to experimental investigation. The approach taken in the early work was to use theoretical considerations as a guide for the experimental investigations. It was decided that the use of argon as a working gas would facilitate the initial experimental investigations. Many of the source characteristics were determined from the theoretical concept of the ion source, such as space-charge-limited current, final ion velocity, specific impulse, propellant flow rate, ion velocity at the slit, and approximate density and pressure at the exit slit. The ionization phenomena within the cavity were investigated theoretically in regard to the ion production rate and ion losses to the chamber walls. The wall loss is determined by ion transfer to the sheath at the magnetic pole face. The requirements of the magnetic field within the source were determined by an analysis of electron diffusion across a magnetic field.

The theoretical analysis of the transverse field ion source was applied to the design and construction of a 4.5-inch diameter experimental model. The basic mechanical configuration of the experimental model ion source is shown in Figure 2.1.1. A photograph of the completed assembly is shown in Pictorial 2.1.1.

The operation of the ion source is dependent upon a magnetic circuit, an anode to cathode potential drop, a hot cathode, and an extraction system. The magnetic circuit design was based on theoretical estimates of the fringing losses and on the reluctance of the exit aperture gap. The aim of the design was to insure that a field strength of at least one kilogauss would be available in the vicinity of the exit aperture. The magnet windings were provided with water cooling to dissipate heat generated in the windings. To facilitate the cooling, an open type of winding was used which allowed free circulation of water to all turns. The cooling water flow pattern was designed to be self-purging, so that gas bubbles could not accumulate and cause local hot spots. A vacuum seal between the cooling water and the arc chamber was made by soldering a large brass washer over the end of the magnet winding region. Mild steel was used in the construction of the magnetic circuit and the magnetic field was shaped in the arc region by the beveled pole faces.

The anode was constructed in the form of a brass ring with a V-shape groove present around the ring. Propellant (argon) was brought into the arc region by way of a propellant supply tube through the mild steel engine wall. The propellant

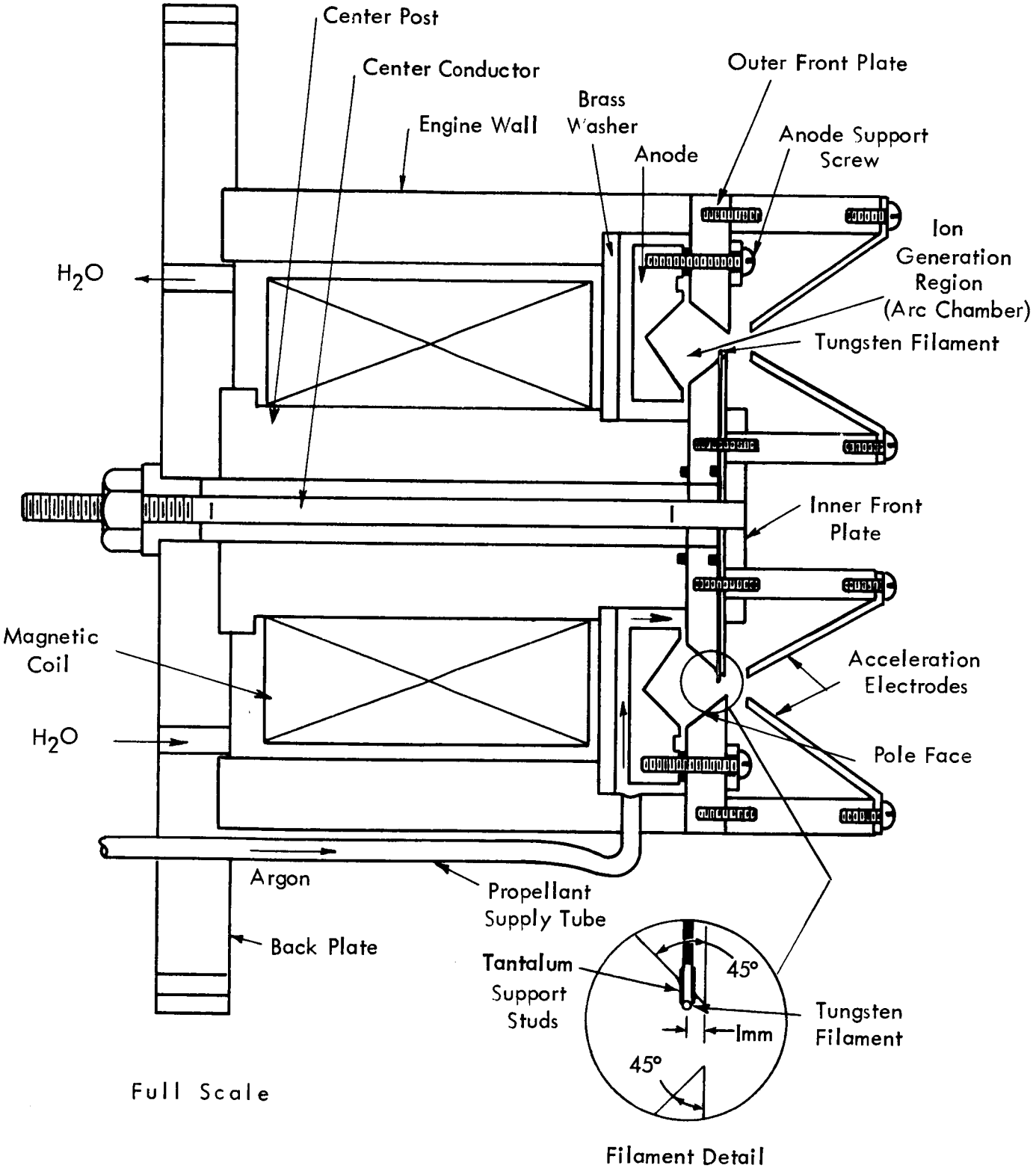


FIGURE 2.1.1 INITIAL RESEARCH MODEL CONFIGURATION (CROSS SECTION VIEW)

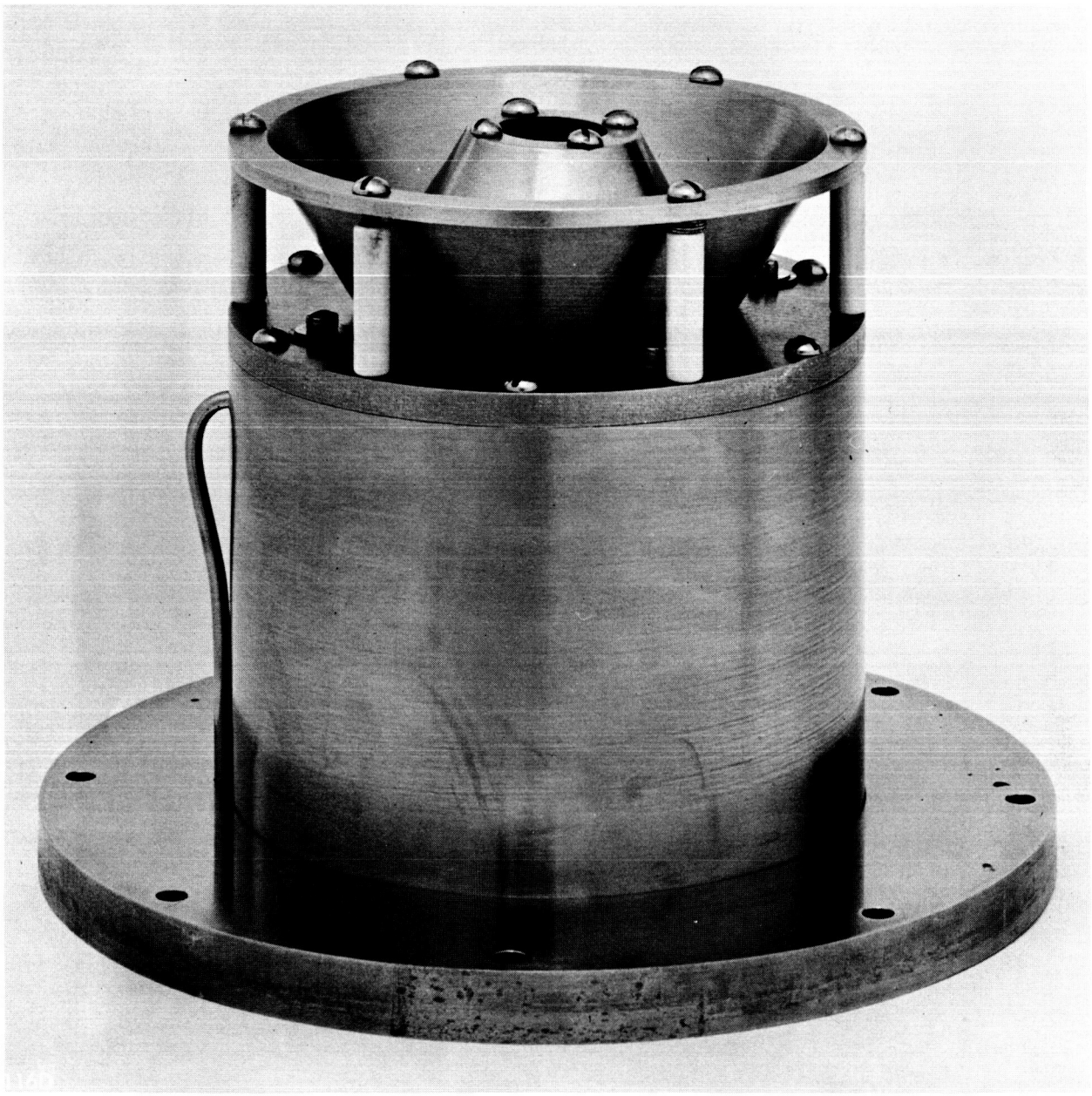

PICTORIAL 2.1.1
INITIAL RESEARCH TEST MODEL

diffused around the anode to the arc region. The anode potential was obtained by an electrical connection to a support screw through the front of the ion source. The cathode structure was a simple tungsten filament heated by electrical current passing through the center conductor, along the front plate, through the filament, and then back to ground. A parallel electrical connection was necessary to keep the AC voltage drop across the cathode small compared with the arc potential.

Since the primary work to be performed with this source dealt with the source rather than the beam accelerating system, the source was operated near ground potential and a simple acceleration electrode structure was utilized. This arrangement greatly simplified electrical measurements, but also required operating the ion beam acceleration system and target at high negative potential. To prevent deflection of the ion beam by ground potential surfaces in the vacuum tank, it was necessary to provide electrostatic shielding for the beam.

### 2.1.1 Source Optimization

The experimental model ion engine was installed in the 3 ft x 5 ft vacuum test facility depicted in Pictorial 2.1.2. Other equipment such as a calorimeter target, electrostatic shield, and power supplies were set up. The instrumentation for the source consisted of metering for all voltages and currents, plus a propellant flow rate meter and a beam power calorimeter. The calorimeter was quite simple and reliable, consisting of a thick disc of aluminum. The disc constituted a thermally insulated mass of known heat capacity. Its temperature was measured utilizing a mercury thermometer before and after a period of source operation, and its temperature rise was correlated with the time integral of the electrical beam power. An initial performance analysis was conducted over a wide range of conditions (flow rates) to establish a desirable operation region. It was found that the magnitude of the magnetic field influenced the output ion beam current. An optimum magnetic field strength condition was observed and data was taken only at the determined optimum magnetic field strength during the initial experimentation. Tests were also made to determine the proper voltage for the calorimeter target in order to suppress secondary electrons. The source to acceleration electrode spacing was adjusted to give a well-focused ion beam. Data of the transverse field ion engine operation was obtained under good focusing and secondary electron suppression conditions. The results showed the general performance characteristics of the ion source although the efficiency of operation was not good. The effort was, therefore, directed toward improving the operating efficiency.

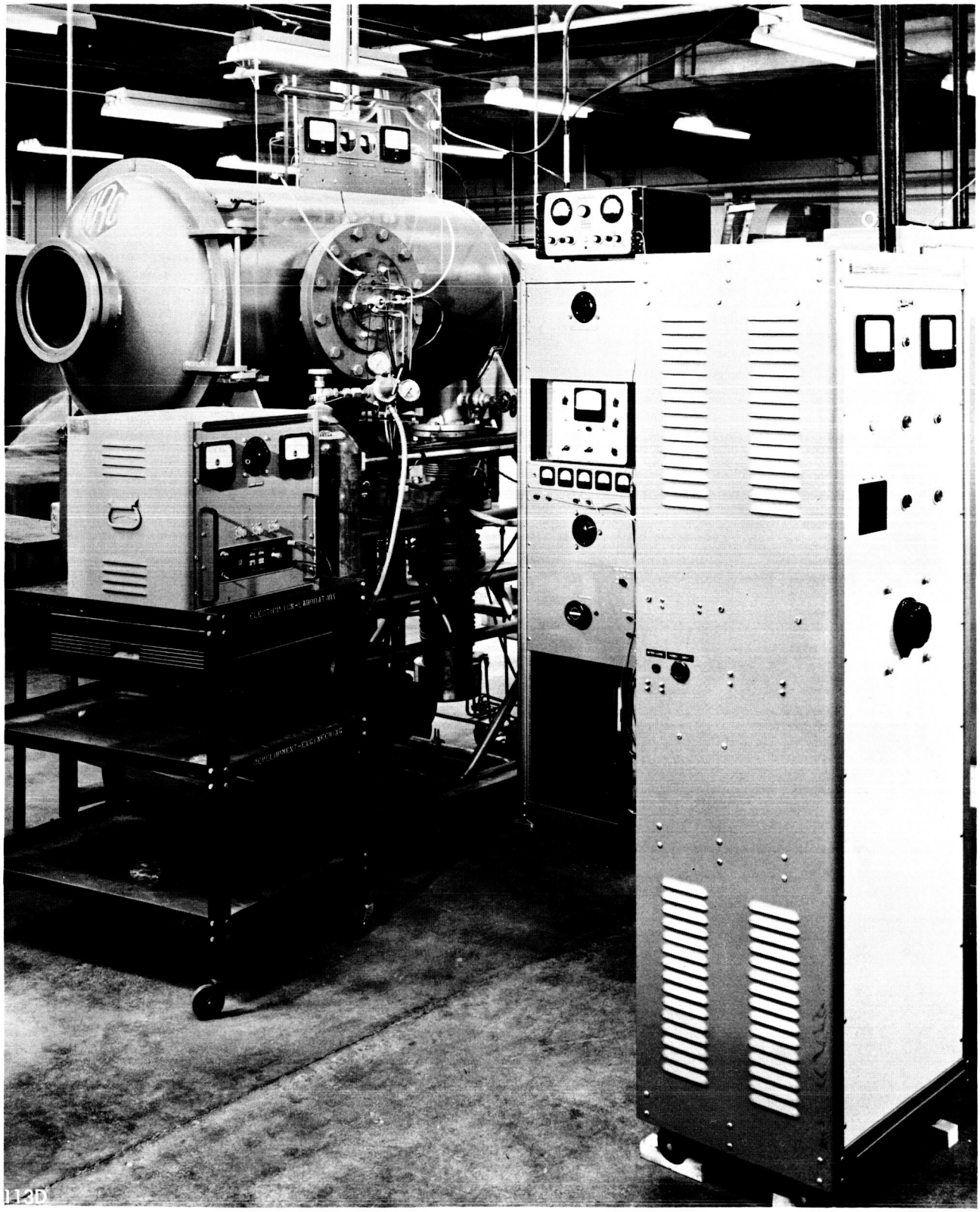

PICTORIAL 2.1.2
INITIAL RESEARCH FACILITY

Several modifications of the ion source were made in the attempt to improve the efficiency of operation. The cathode position was altered and it was found that the original position was close to the optimum (optimum position shown in Figure 2.1.1). The effect of the anode spacing was investigated and it was found that smaller anode spacings required a higher chamber pressure (higher argon flow rate) for optimum ion source operation. The reason for the difference in chamber pressure was due to the longer electron path for the larger anode spacings which allowed the same number of electron-atom collisions in the lower pressure region as occurred in the shorter, higher pressure region.

There was an insulator (Sauereisen) applied to the pole faces for the experiments and the possibility existed that the insulator was poisoning the discharge. The insulating material had been applied in an attempt to define the boundary field conditions. The ion source operation was tested with the insulating material removed from the pole faces and improved performance was noted (40 per cent propellant utilization, 700 eV/ion ionization inefficiency). The insulating material had been entering the discharge and poisoning the arc. The performance of the ion source improved as the propellant flow was increased. The ion beam was well focused, power transfer was calorimetrically verified, and good secondary electron suppression was obtained. The annular shape of the ion beam was evident from the erosion pattern on the calorimeter. Pictorial 2.1.3 shows this effect. The experimental results indicated that higher propellant flow and a larger arc chamber would give improved performance. It was then decided to relocate the experiment in a larger vacuum system, 7 ft x 12 ft, so that larger propellant flow rates could be investigated. A new air cooled calorimeter was also constructed since prolonged ion source operation caused excessive heating of the uncooled calorimeter.

Tests of the ion source performance were made in the large vacuum facility for several anode spacings. It was found that the anode to cathode spacing had little effect upon the source operating efficiency when the flow rate was varied inversely with the anode to cathode spacing. From a theoretical point of view, a change in spacing merely changes the length of the positive column and has little effect on the efficiency of operation if the number of electron-neutral encounters was kept the same. A 45° pole face angle was used in this investigation, as in the previous experimental work, and data in the 700 eV/ion and 40 per cent propellant utilization region was obtained.

The next step in the experimental investigation for ion source efficiency optimization was to investigate the pole face sheath conditions and the focusing electric

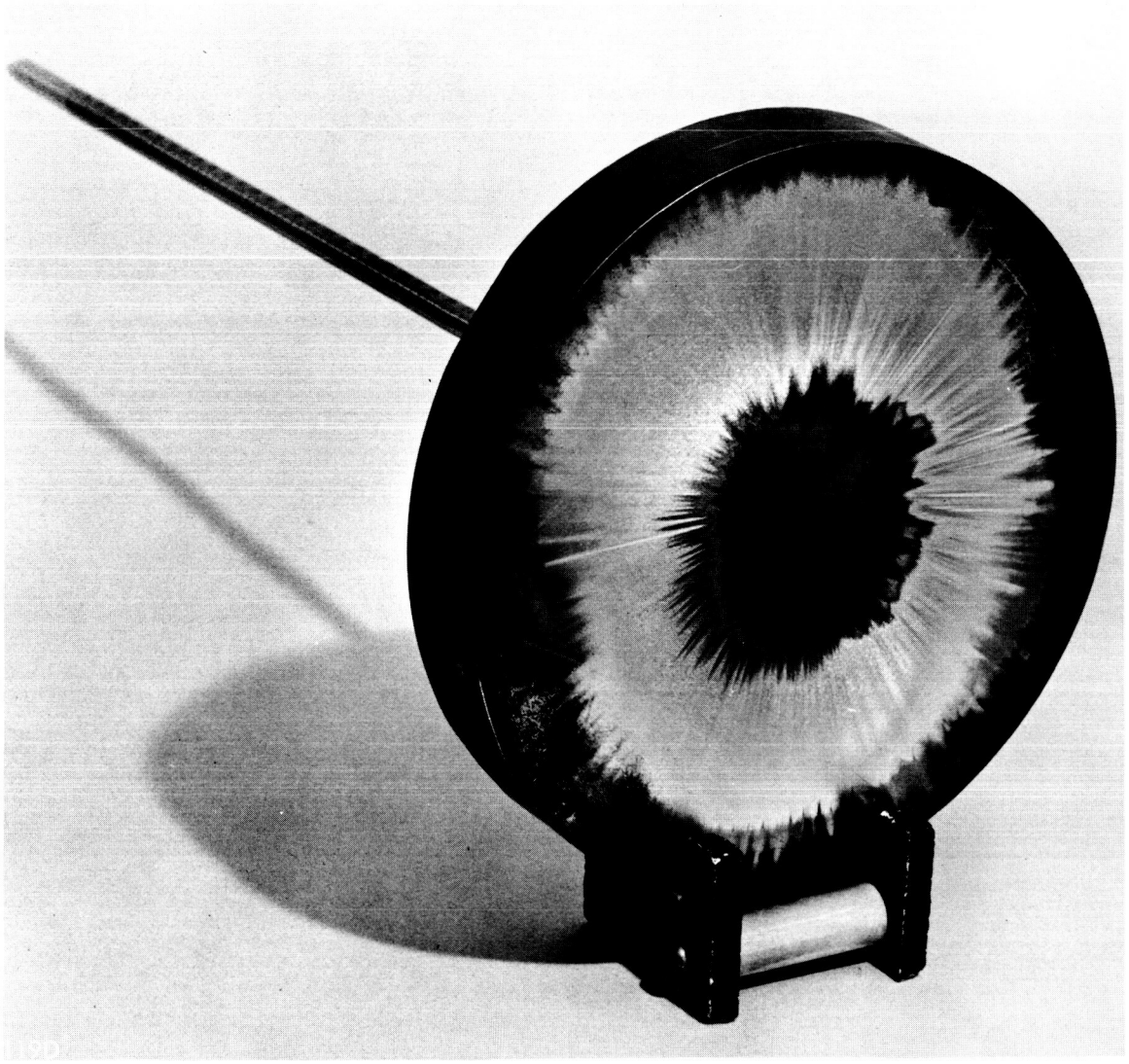

PICTORIAL 2.1.3
CALORIMETER EROSION DETAIL

field as a function of the pole face angle. It was determined theoretically that smaller pole face angles would give improved operation. The improved operation would occur from better focusing of the electric field near the exit aperture. This effect is shown in Figure 2.1.2. The equipotential lines form a better approximation to a semicircle near the exit for the smaller pole face angle. Ions flow in a direction perpendicular to the equipotential lines and fewer ions will be lost to the walls for the smaller pole face angle. Also, the greater inhomogeniety of the magnetic field near the exit aperture will cause a steeper potential gradient (the equipotential lines are influenced by the magnetic field through the electron motion) and the ions will experience a larger magnitude electric field which will pull the ions out of the source. Experimentally, the pole face angle was first changed to 30° and the ion engine performance was checked. Improved operation was obtained, typically 700 eV/ion arc efficiency at 45 per cent propellant utilization. A 15° pole face angle was tried and it was found that the cathode posotion became quite critical in its influence on the ion source operation. An optimum cathode position was experimentally found (the optimum position was in line with the pole face points right at the exit aperture) and ion source performance in the 450 eV/ion arc efficiency and 60 per cent propellant utilization region was obtained. The performance data is shown in Figure 2.1.3. This data was verified by calorimeter measurements. Further decreases in the pole face angle were not made due to mechanical requirements.

The cathode position was varied to determine the effect of the cathode position upon the ion source operation. Positions tried were 1.4, 1.0, 0.6, 0.5, 0.4 and 0.0 mm behind the line joining the inner and outer pole piece points. The optimum positions were between 0 and 0.5 mm suggesting that the electrons should be introduced to the plasma where the maximum magnetic field existed. This behavior agreed with theoretical expectations.

The final parameter variation made with the initial experimental model was the variation of the exit aperture size. Tests were made at exit aperture openings of 0.6, 0.8, 1.0, and 1.4 mm. Arc performance combined with the least mechanical problem of filament location was best at exit aperture openings of 1.0 and 1.2 mm. The smaller exit aperture openings made the mounting of the filament (without subsequent electrical shorting) a difficult problem. Exit aperture sizes larger than 1.4 mm caused a problem in that the extraction potential altered the arc conditions. Shielded cathode configurations were investigated to limit the acceleration voltage influence on the arc potential. A limited amount of shielding was

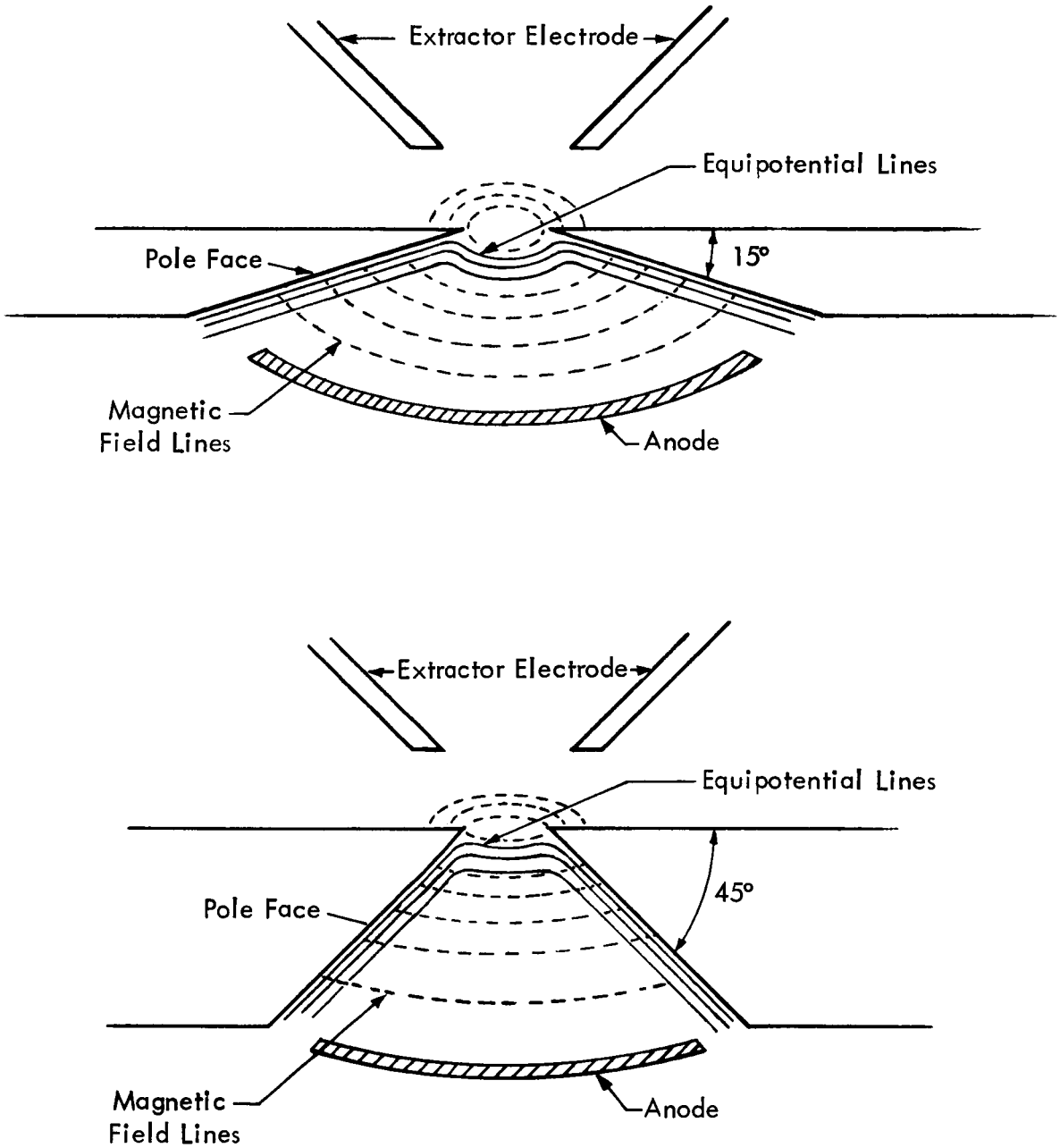


FIGURE 2.1.2 FIELD DEPENDENCE ON POLE FACE ANGLE

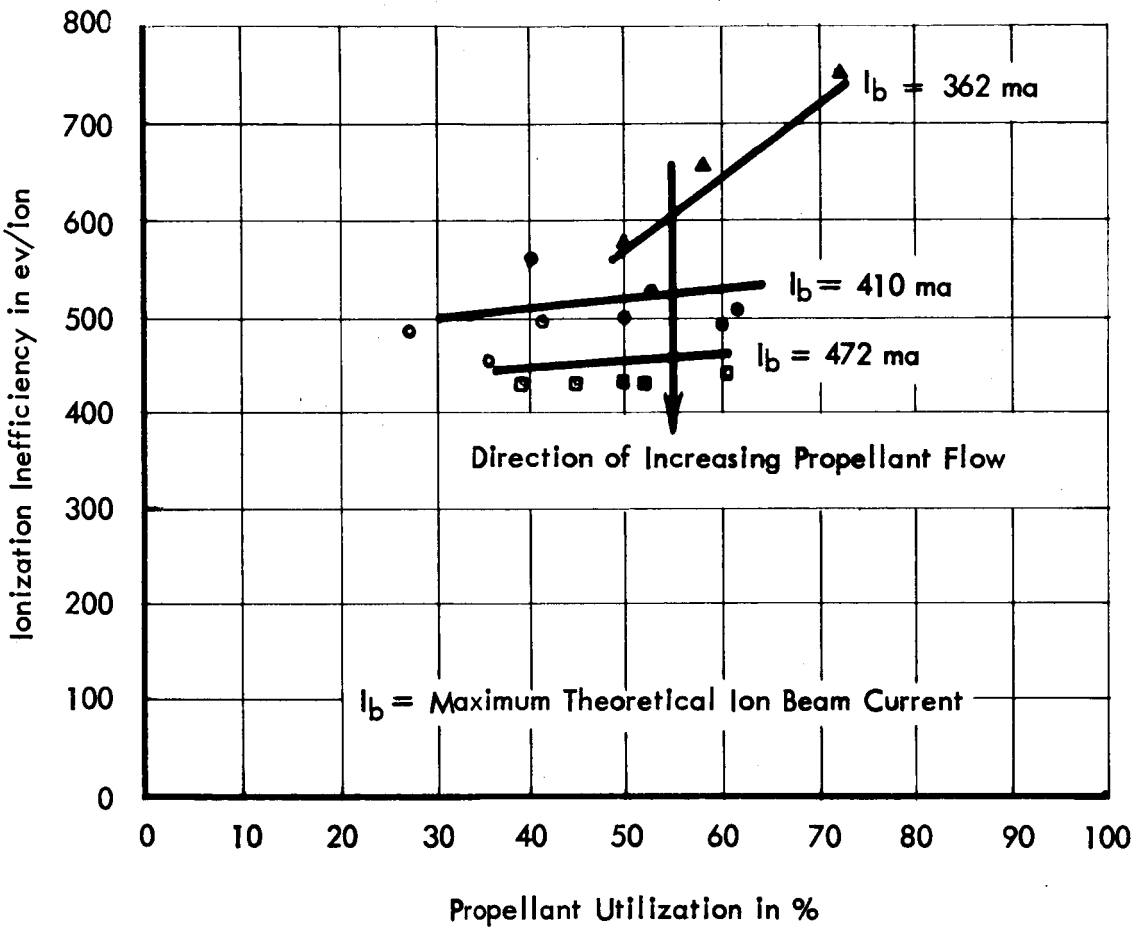


FIGURE 2.1.3 PERFORMANCE CHARACTERISTICS OF INITIAL RESEARCH MODEL

beneficial although it was necessary to maintain good exit aperture field conditions and also allow the cathode to be in intimate contact with the plasma.

### 2.1.2 Seven-Inch Diameter Ion Source (Argon Propellant)

The performance characteristics of the initial research test model had supported the basic theory and promise of the transverse field ion source. However, further improvements in the arc efficiency were desired. The theoretical way to improve the arc efficiency was to lower the chamber pressure (decrease ion-electron recombination losses) and to increase the chamber size so that a more copious electron supplier (larger tungsten wire) could be installed. An enlarged arc chamber was constructed. A cross section view of the arc chamber is shown in Figure 2.1.4. This new configuration was tested with a larger diameter cathode (three twisted 0.005-inch diameter tungsten wires) and a significant improvement in operation was noted. Tests were performed to show the variation of the ion engine performance with propellant flow rate. An optimum flow rate corresponding to 893 ma of theoretical ion beam current was found. Figure 2.1.5 shows the experimental results which were obtained. The arc conditions indicated that a sufficient number of electrons were present to allow efficient ionization of the argon propellant.

The ion focusing fields within the ion source appeared to be operating in a manner substantiating the theoretical expectations. No ion bombardment was observed on the outer pole face and very little ion bombardment was observed on the inner pole face (cathode location). The cathode was mounted on the inner pole face and some field perturbations were caused by the cathode's presence there. The operation of the ion source appeared to approximate the desired operating characteristics so the research effort was temporarily diverted to a diagnostic investigation of the plasma characteristics to obtain a greater understanding of the plasma behavior.

### 2.1.3 Diagnostics for Argon Propellant

The electron energy group of interest in the plasma is the high energy group which basically has an energy level corresponding to the cathode fall potential. It is these high energy electrons which are responsible for the major portion of the ionization that occurs. The region in the arc chamber where the high energy electrons lose energy may be inferred as being the region where ionization occurs. The transverse field ion engine had been developed sufficiently so that efficient ionization was obtainable in the plasma. Theoretically the ionization should occur near the exit aperture for good ion source efficiency. This prediction was to be verified experimentally.

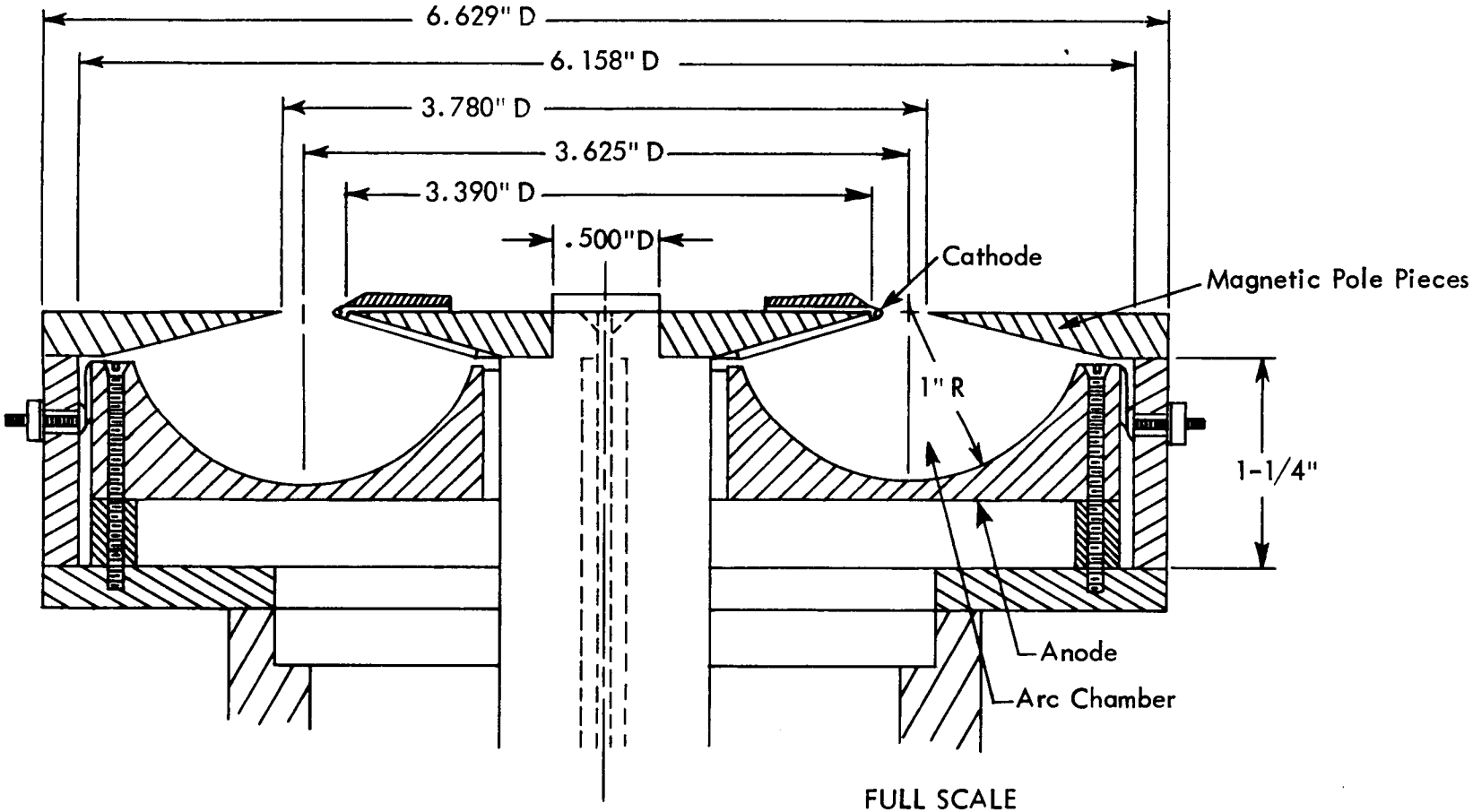


FIGURE 2.1.4 THE ENLARGED ARC CHAMBER DETAIL
(CROSS SECTION VIEW)

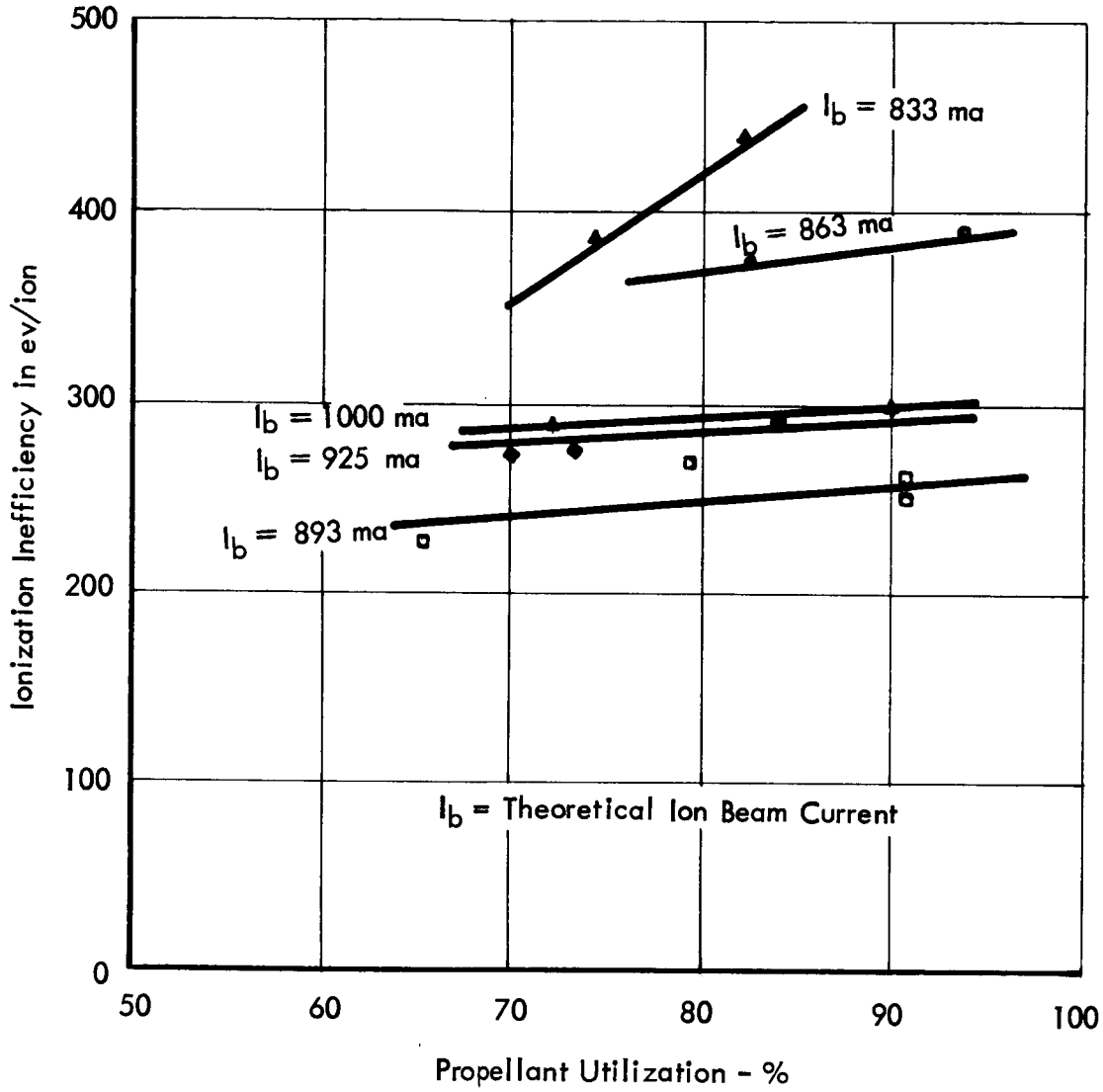


FIGURE 2.1.5 PERFORMANCE CHARACTERISTICS OF THE TRANSVERSE FIELD ION SOURCE WITH THE ENLARGED ARC CHAMBER

The location of the ionization region was determined with a movable probe. The energy of the high energy electron group may be inferred by observing the probe voltage-current characteristics. A typical probe voltage-current characteristic is shown in Figure 2.1.6. When the probe voltage is made very negative, there is a saturated positive ion flow to the probe. When the probe is made less negative, the high energy electrons can reach the probe and the curve begins to have a positive slope. As the probe voltage increases in the positive direction, more of the lower energy electrons are collected, the electron current to the probe surpasses the ion current to the probe, and the total current from the probe becomes positive. Finally for high positive values of probe voltage, saturation of the electron current develops and all the available electrons are collected. The potential difference between the probe voltage when the first few high energy electrons were collected is a measure of the energy of the high energy electron group. This potential difference value is easily obtained by measuring the potential change between the two knees of the probe curve.

A movable probe assembly was designed, fabricated, and tested. This probe assembly was installed in the ion source so that an estimate of the electron energy distribution and magnitude and also the plasma potential distribution could be determined. The probe construction is shown in Figure 2.1.7 and Pictorials 2.1.4 and 2.1.5. The probe had two motions which allowed the probe tip to reach every point of the arc chamber cross section. The horizontal and vertical motions were transmitted through the vacuum system wall with an arrangement of bellows. The probe position could be changed while an experiment was in progress by moving the bellows linkage. The bellows linkage was calibrated to allow accurate remote control positioning of the probe tip. Pictorial 2.1.6 shows the entire unit.

An electrical circuit was designed and constructed to allow the probe curves to be displayed on an oscilloscope. The circuit is shown in Figure 2.1.8. In the figure, an AC voltage signal is impressed upon the probe by the variac. The DC voltage level of the probe is established by a DC voltage supply. The AC driving voltage is displayed on the horizontal plates of the oscilloscope and thus gives the oscilloscope horizontal axis the probe voltage label. The voltage curve for the oscilloscope vertical axis is obtained from the voltage across a 100 ohm resistor in the return leg of the circuit. This last voltage is proportional to the probe current and the proportionality allows the vertical axis to be calibrated to indicate probe current.

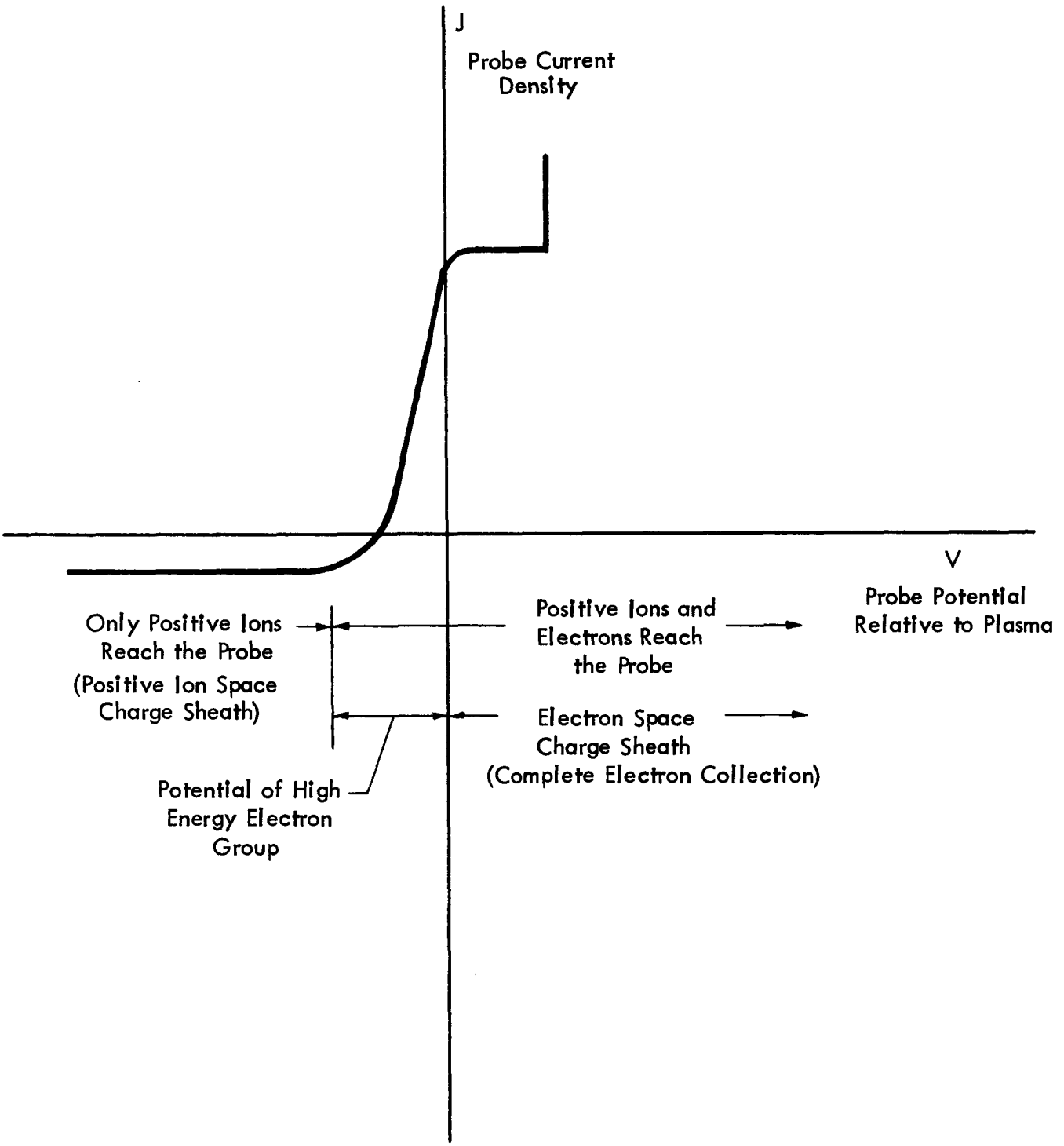


FIGURE 2.1.6 TYPICAL PROBE CHARACTERISTIC CURVE [5]

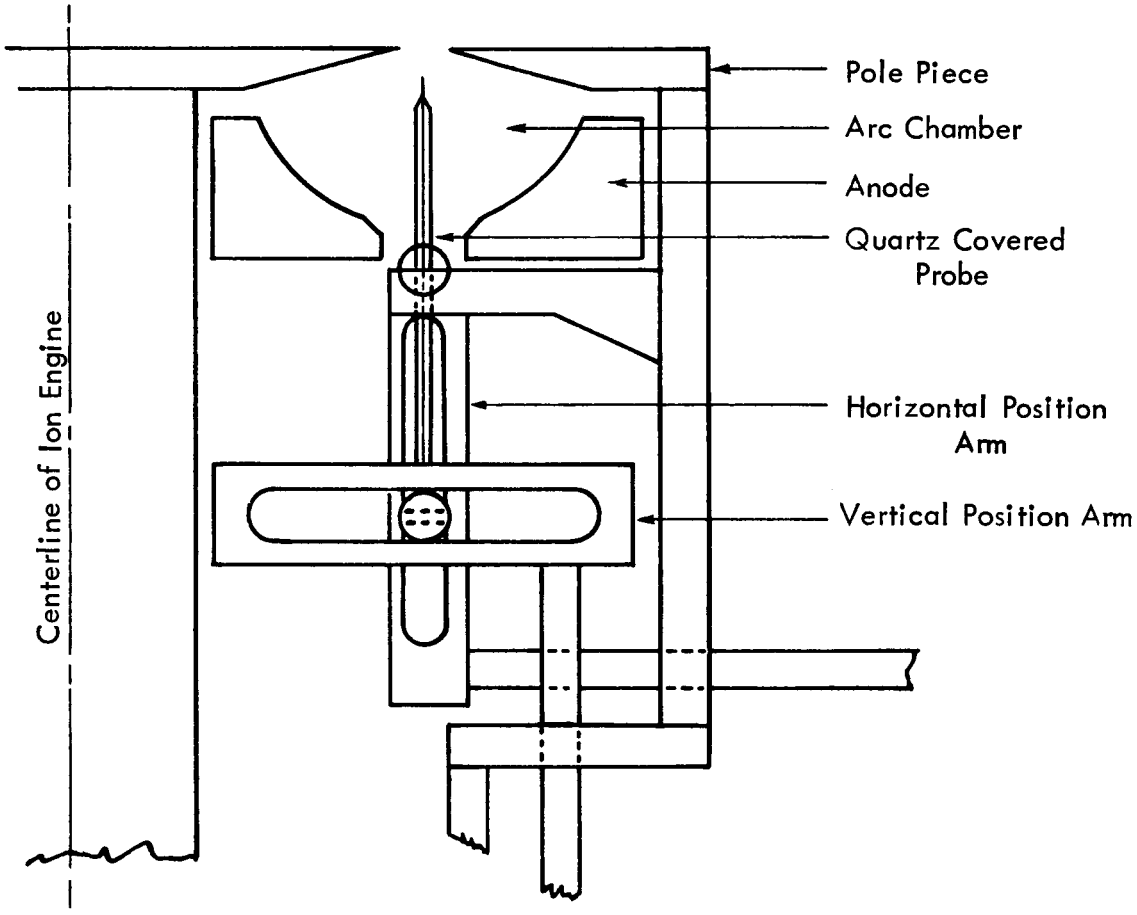


FIGURE 2.1.7 PROBE CONSTRUCTION CROSS SECTION

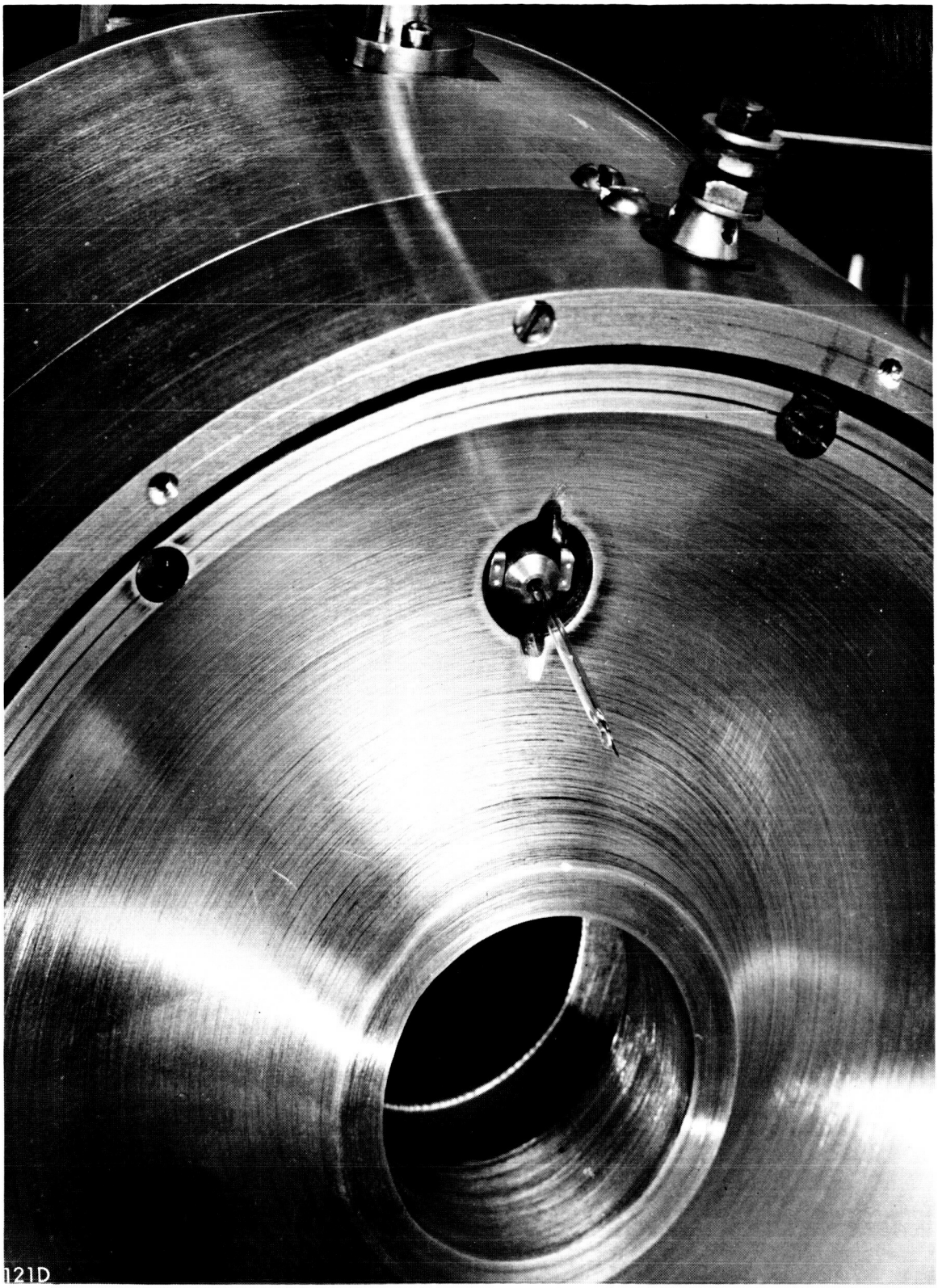


PICTORIAL 2.1.4
PROBE DETAIL

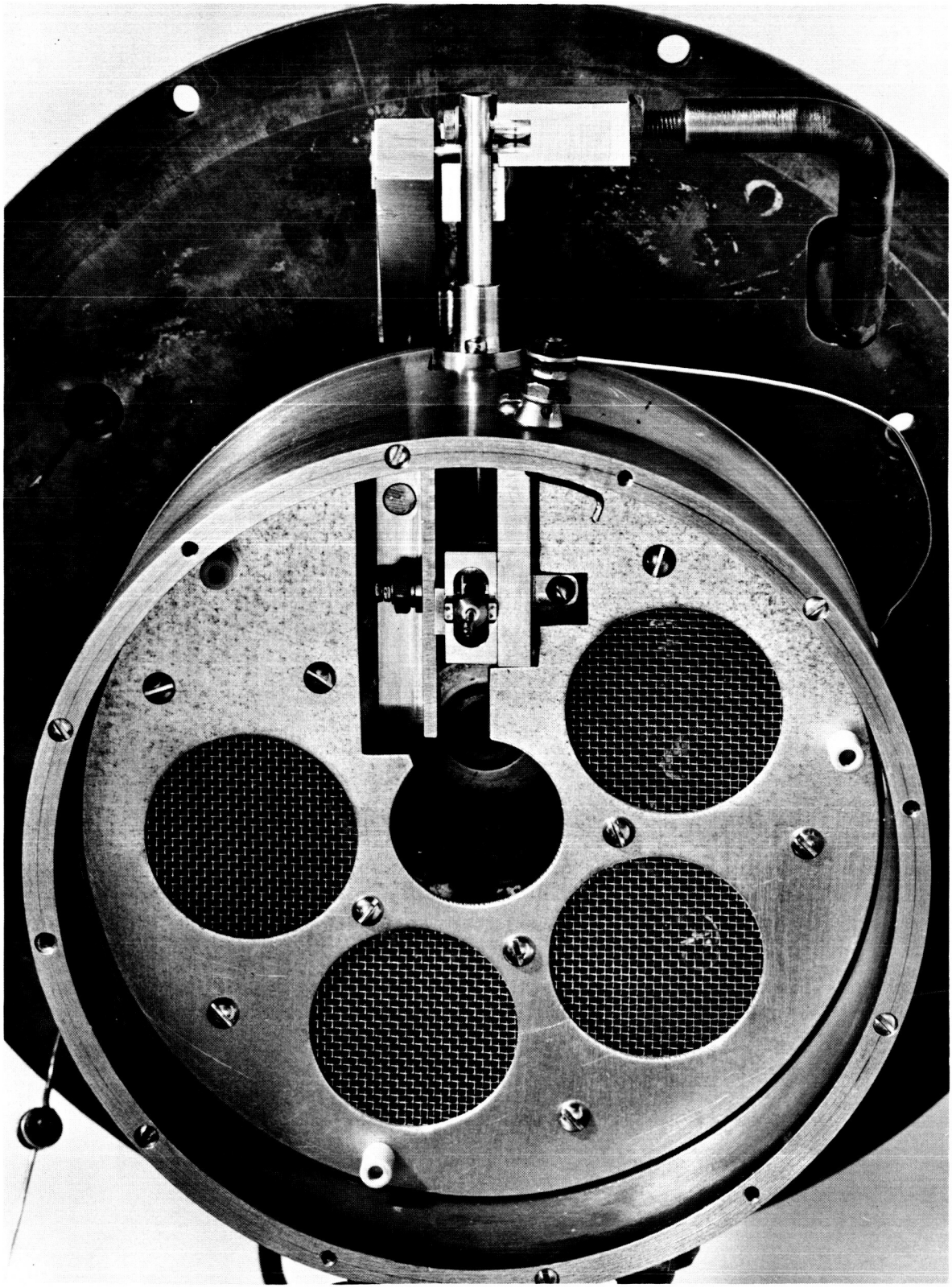

PICTORIAL 2.1.5
PROBE LINKAGE

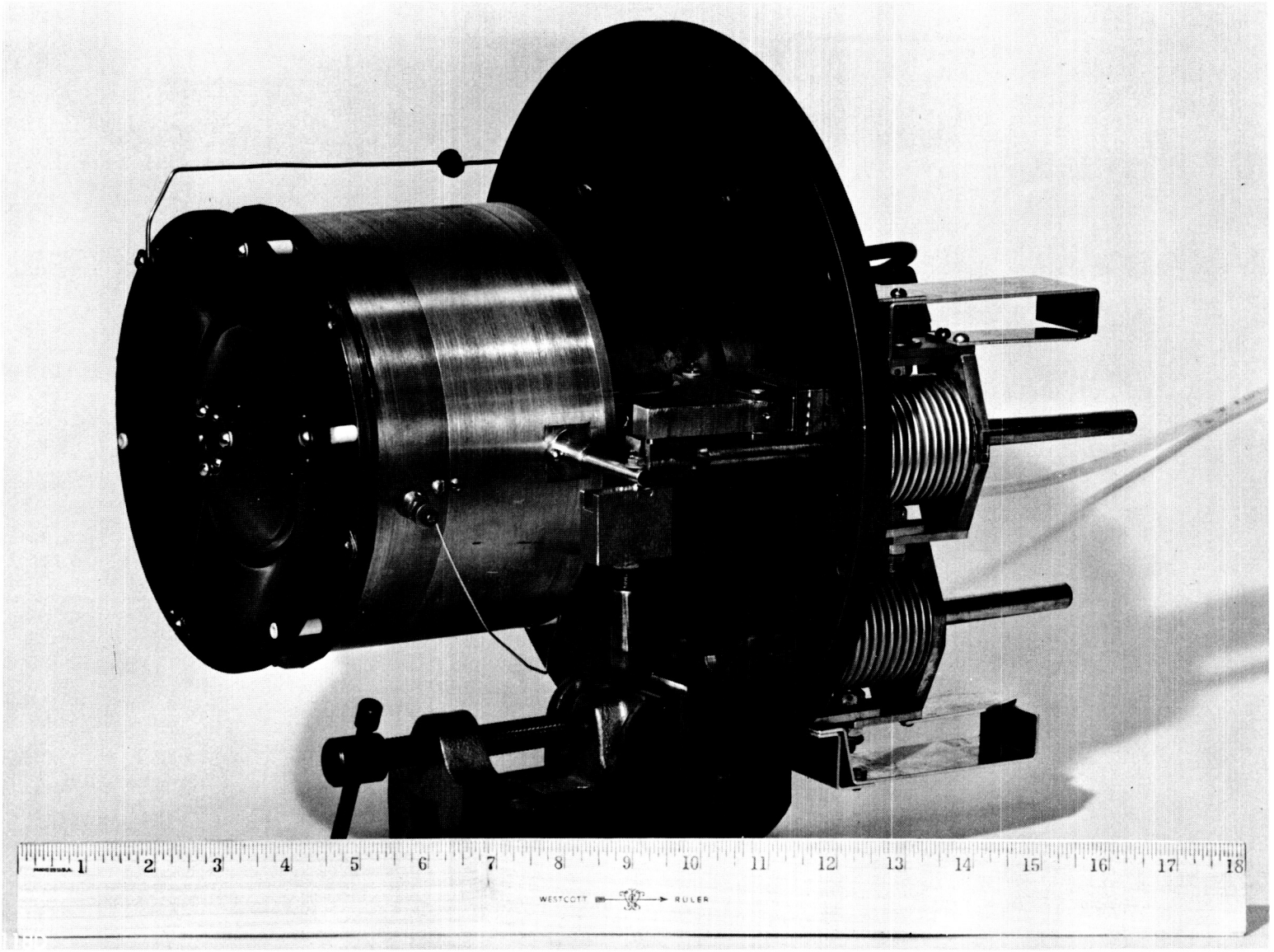


PICTORIAL 2.1.6
DIAGNOSTIC TEST MODEL

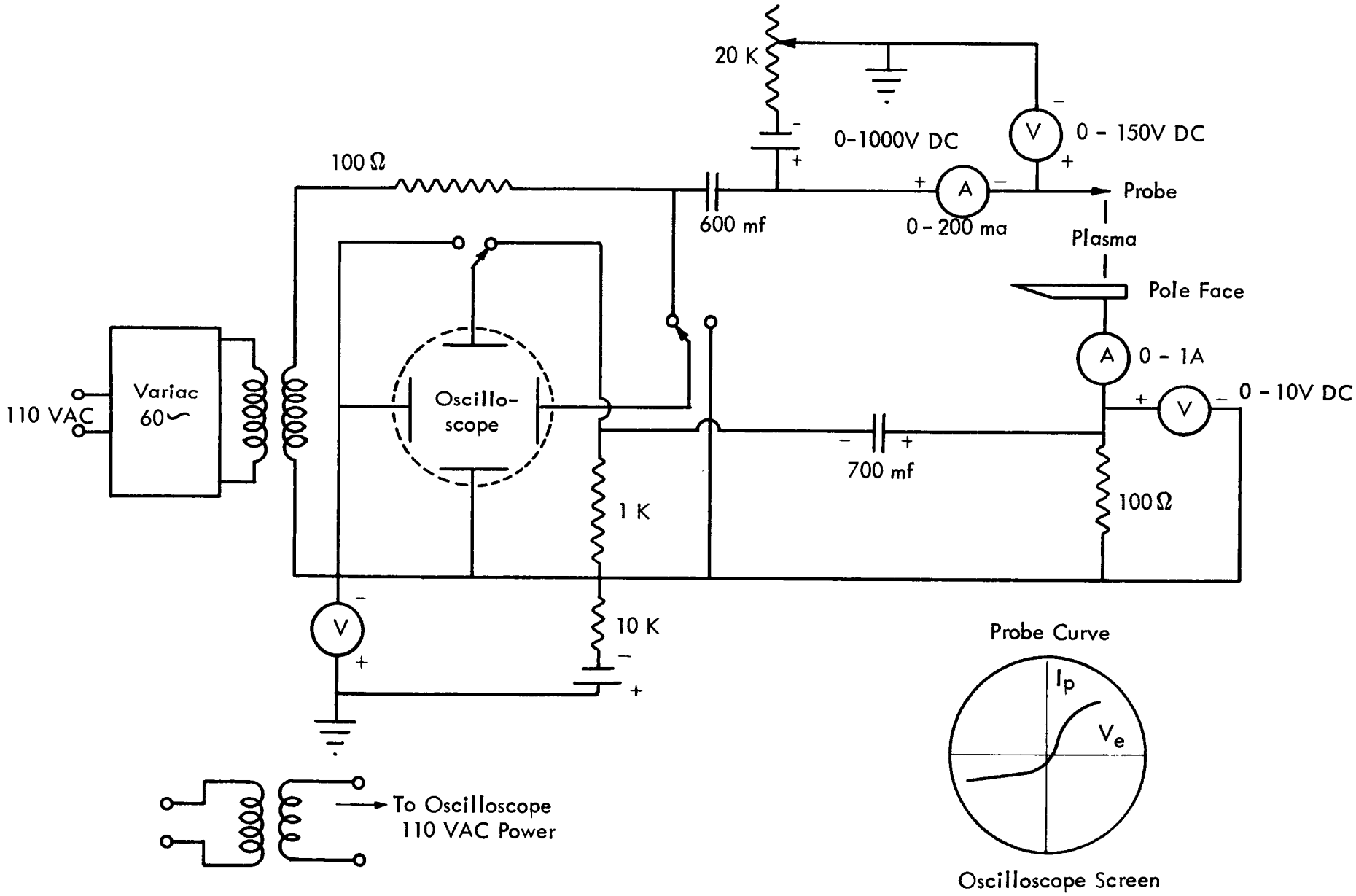


FIGURE 2.1.8 PROBE ELECTRICAL CIRCUIT

Tests of the arc performance were made and data was obtained relative to electron energy and potential distributions within the plasma. The high energy electrons had a spacial energy distribution along the axis of the arc as shown in Figure 2.1.9. The high energy electrons are the electrons of interest since they are the main source of ionization in the discharge. The high energy electrons lose a significant amount of energy in the first few millimeters near the exit aperture which suggests a substantial ion production in that region. The ion source performance level for this operation was 200 to 250 eV/ion arc efficiency at 95 per cent propellant utilization (argon propellant). The plasma potential was nearly constant along the axis of the arc which indicated a high degree of ionization (high plasma conductivity). The plasma potential was nearly identical with the anode potential from the anode to the exit aperture. Further probe studies appeared unnecessary at this time since the important plasma characteristics for good ion source operation had been determined.

### 2.1.4 Seven-Inch Diameter Ion Source (Mercury Propellant)

The successful operation of the transverse field ion source with an argon propellant had been completed so it was decided to attempt to operate the transverse field ion source with a mercury propellant. The previous experimental and theoretical knowledge which had been obtained from the argon operation was applied to predicting the operating characteristics of the ion source with the mercury propellant. It was decided to use the same experimental ion source for initial experimentation. Optimum performance was predicted for mercury flow rates corresponding to approximately 450 ma of ion beam current.

The conversion from argon to mercury required the construction of a mercury feed and vaporization system. The feed system consisted of a precision mechanical drive which delivered mercury at a uniform rate to the vaporizer. The flow rate was easily adjustable. The vaporizer was a porous stainless steel plug into which the mercury was driven. A temperature gradient was maintained along the plug. The vapor evolving from the plug was directed through heated tubing to the ion source.

A cold trapping system was utilized in the vacuum chamber to protect the vacuum pumps from mercury contamination. The system had been constructed under Contract NAS8-42 and consisted of a large area of cooled copper sheet and tubing inside the vacuum chamber. Cooling was accomplished by pumping liquid nitrogen through the copper tubing attached to the copper sheet.

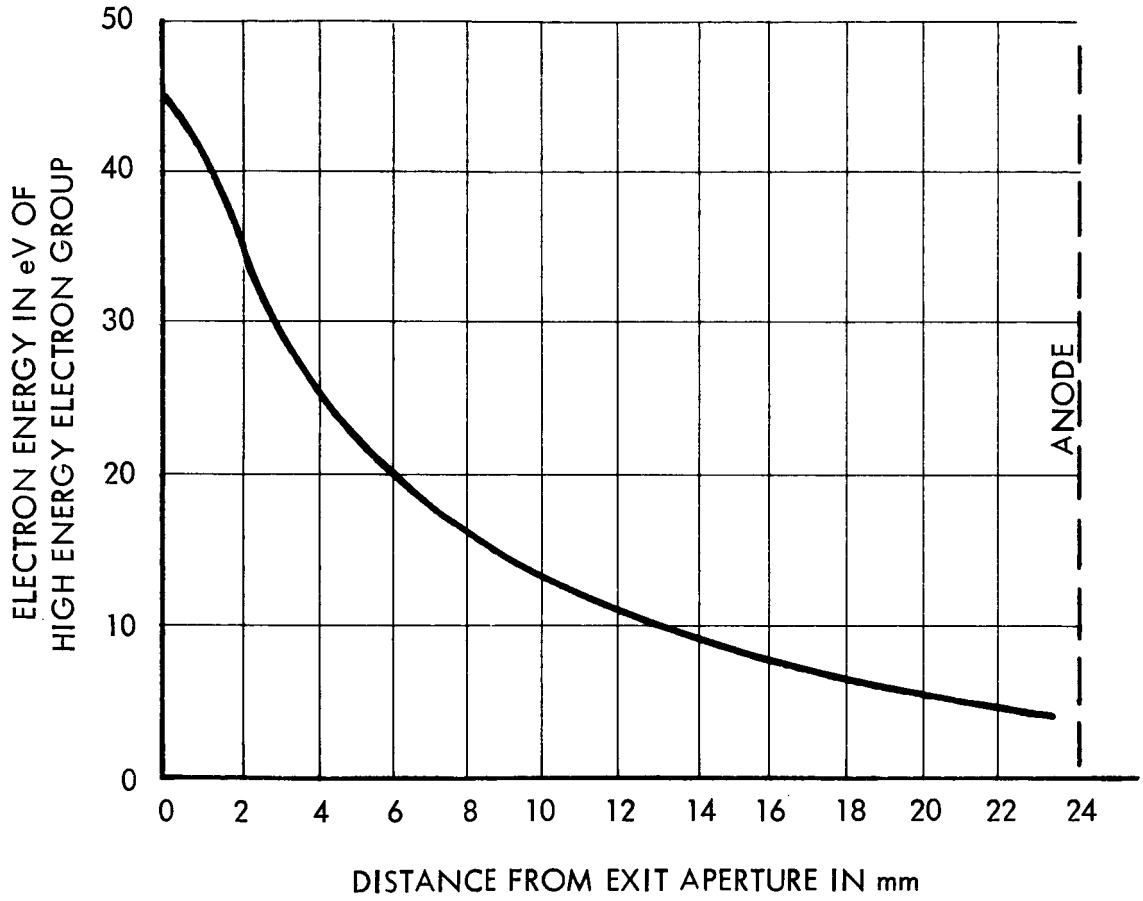


FIGURE 2.1.9 ELECTRON ENERGY DISTRIBUTION

The ion source alterations which were necessary for the conversion to mercury propellant were not extensive in nature, but they did give rise to certain operational problems. The basic changes consisted of coupling the source to a heated mercury vapor transfer tube and providing heat to the source itself to prevent mercury condensation. Coupling the source to the transfer tube presented no great problem. The tube, which carried mercury vapor from the external vaporizer through the vacuum wall and into the source, was heated electrically to prevent condensation and consequent uncertainty of the propellant flow rate. The mercury supply system operated satisfactorily from the time it was installed, requiring only sufficient testing to establish flow equilibrium times at the flow rates used. Operating the source at elevated temperatures was accomplished by passing steam through the magnet coil box. A special portable steam generator was acquired for this purpose.

Tests were made of the ion source performance with the mercury propellant. The initial test was quite successful and the arc efficiency and propellant utilization characteristics were determined for several flow rates. The arc efficiency versus propellant utilization is shown in Figure 2.1.10. The cathode power was approximately 500 watts which was too high for practical ion source operation. Three twisted 0.005 inch tungsten wires formed the cathode which was electrically heated.

Qualifications should be stated to restrict optimistic conclusions from the curves of Figure 2.1.10. The propellant supply system was not as refined as those developed later in the program. Therefore, an error in mercury flow rate was possible. Also high arc voltage (35 to 40 volts) in the high propellant utilization region presented the possibility of the presence of doubly ionized mercury ions in the ion beam. These qualifications should be considered to prevent overestimating the capabilities of the source performance.

The general source performance appeared encouraging within the limits stated above. It was evident that further experimentation should take the form of a refinement of the propellant, acceleration, and cathode systems. The first significant milestone, the achievement of good arc efficiency with a mercury propellant, had been reached. The behavior of the ionization process and the plasma characteristics had been well established and the experimental arc efficiency had substantiated the theoretical promise of the transverse field ion source.

The remaining major problems to be solved were to develop an efficient cathode and an extraction system for the transverse field ion engine. A preliminary investigation into the cathode problem was begun. Thoriated tungsten cathodes or nickel

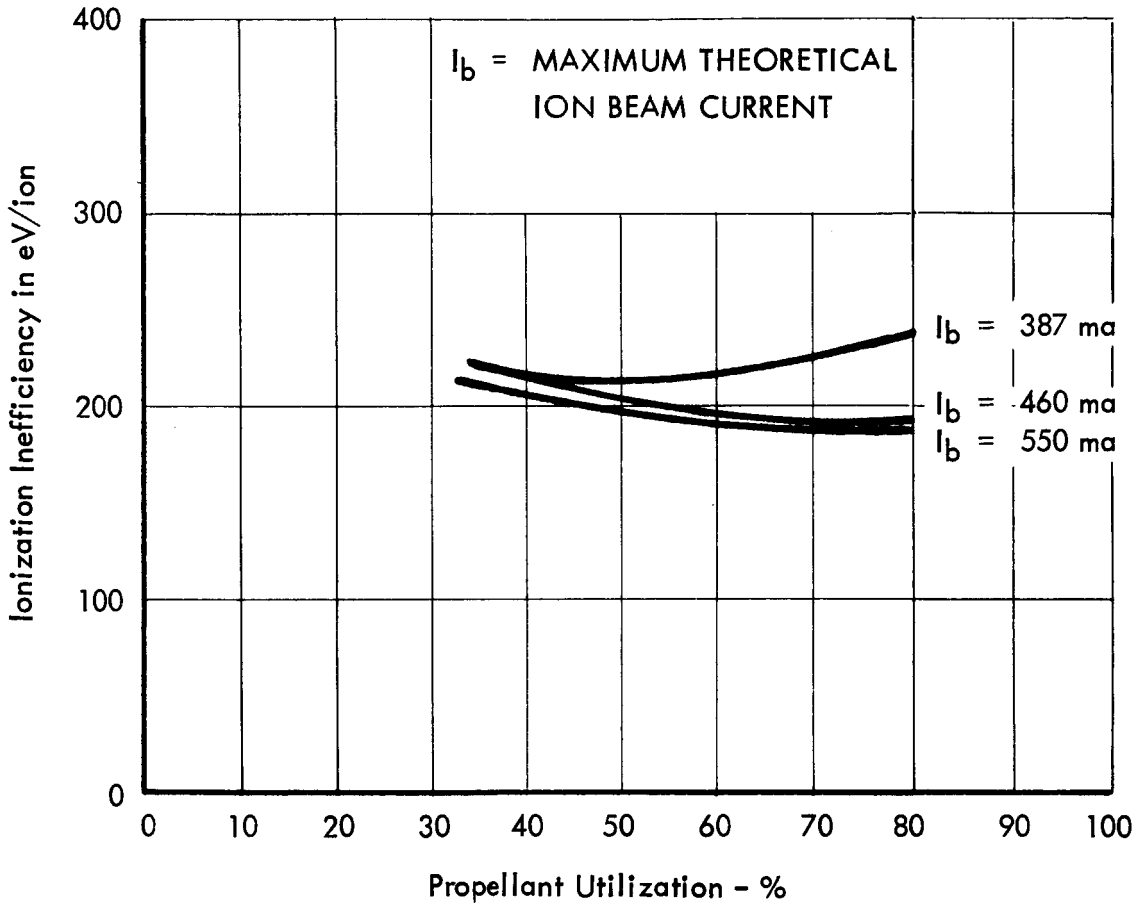


FIGURE 2.1.10 PERFORMANCE CHARACTERISTICS WITH A MERCURY PROPELLANT

matrix dispenser cathodes appeared to be possible answers to the problem of decreasing the cathode power while maintaining a sufficient electron supply to the discharge. Thoriated tungsten cathodes operate at a lower temperature than pure tungsten cathodes and have an emission efficiency of 25 to 80 ma/watt compared with 2 to 6 ma/watt for pure tungsten. Comparison with pure tungsten cathode operation indicates that sufficient numbers of electrons could be obtained from the thoriated tungsten cathode at power expenditures of 50 to 100 watts. This would correspond to a 100 to 200 eV/ion decrease in the efficiency. The lifetime performance of a thoriated tungsten cathode depends upon the cathode configuration and the maintenance of the arc voltage below 22 volts. The arc voltage requirement is necessary to keep the thorium monolayer from being sputtered away by positive ion bombardment. This arc voltage requirement makes the use of thoriated tungsten cathodes in the transverse field ion source questionable since it may be difficult to obtain a high propellant utilization at such a low arc voltage.

A thoriated tungsten cathode was installed in the ion source. The cathode consisted of a 0.005-inch diameter, one per cent thoriated tungsten wire which was mounted on 0.025-inch diameter tantalum support studs. Activation of the cathode at temperatures of 2500°F was not accomplished due to the conductive heat loss associated with support studs. At this point, it seemed that the most valuable course of action was to investigate the nickel matrix dispenser cathode for application to the transverse field ion source.

The matrix type dispenser cathode appears to be the most promising cathode for use in a low pressure mercury discharge. The major advantages of the nickel matrix dispenser cathode is that it has a machinable surface, may be exposed to the atmosphere when cool without suffering a diminished emission level in subsequent tests, has a good resistance to ion bombardment and poisoning, and has an adequate lifetime for ion propulsion applications. An initial effort was made to install a nickel matrix cathode in the ion source. The cathode material that was available at that time did not provide adequate electron emission to give the necessary arc voltage and current characteristics. Further work on installing suitable nickel matrix cathodes in the transverse field ion source was deferred until a concurrent investigation of various cathode compositions and sintering techniques (NAS3-2522) was completed.

## 2.2 Extraction Electrode Studies

The next phase of the experimental research was to investigate the problem of developing an efficient and long life extraction system. The objectives of the extraction electrode studies were to investigate the problems associated with the extraction of an ion beam from the transverse field ion source, to establish the criteria for obtaining an ion beam with a suitable specific impulse at satisfactorily low ion impingement on the acceleration electrodes, and to construct a low inpingement extraction system for experimental research purposes.

The accelerating system life problem comes about as the result of the following circumstances.[2] First, a requirement exists to neutralize an ion beam being used for propulsion. If the ions are positive, this neutralization may be accomplished by injecting electrons into the ion beam downstream of the accelerator electrode. It is here that the complication arises, for the ion source is strongly positive relative to the beam potential, so some means must be used to keep the electrons from streaming back to the source.

Virtually the only way in which this can be done is by utilizing an accel-decel system in which the accel electrode is operated somewhat negative with respect to the final electrode and ion beam. The negative potential region is upstream of the neutralizer, effectively preventing electron backstreaming. Maintaining the accel electrode at potentials below the beam potential is the feature which causes the life problem, however, for it is not possible to completely protect it from bombardment by high energy ions.

The ions proceeding directly from the source are not the fundamental problem in this case, for they can always be focused to miss the accel electrode completely. The problem arises from the fact that not only ions are emitted from the source; neutral atoms also are emitted as a result of incomplete propellant utilization. As the neutral atoms drift through the inter-electrode region, some of them become ionized by charge exchange with ions streaming past. These charge exchange ions can, in principle, be focused into the final beam if they are formed in a region above the final beam potential. However, if they are formed below the final beam potential, it is certain that they will strike the accel electrode. Practical considerations render the energies of these ions sufficiently high to do sputtering damage, so it is seen that the accel electrode life can never be made indefinitely long.

There are several approaches to the problem. First, the damage done by the sputtering ions can be reduced as far as possible by operating the accel electrode at a voltage close to the final beam potential. Also, the geometry can be adjusted so that the region below the final beam potential is small, thereby reducing the number of ions formed. A third approach is to reduce the number of charge exchange ions formed by reducing the primary ion current and the neutral atom densities. A fourth way of increasing the life is to direct the bombarding ions to a region of the electrodes that can undergo considerable damage without adversely effecting the operation of the electrode system. A last method of prolonging the life is to utilize a propellant which has a small propensity to form ions by charge exchange.

Generally speaking, all of these measures must be utilized to some degree in order to arrive at an electrode design of adequate life. Most of the methods mentioned are geometric in nature, and we shall discuss them presently. The last measure, however, can be discussed independently of size or configuration, so we shall consider it before the others.

The matter of propellant choice hinges on several factors besides accel electrode life. First, it must be chemically compatible with the propellant feed system materials available, with cathodes, and with engine electrodes. It must also be capable of being metered and vaporized for low power expenditure and it must be efficient from a thrust point of view. This last requirement means that substantially less total energy must be expended in ionizing a propellant atom than in accelerating it. It can easily be seen that this last requisite favors high atomic mass propellants strongly. Since the ions are accelerated electrically, the kinetic energy they acquire equals their charge times the voltage difference through which they have been accelerated. The energy expended to accelerate an ion mass m to velocity v is thus:

$$eV_a = \frac{mv^2}{2} \qquad (2.2\text{-}1)$$

where e is the ionic charge (the electron charge for singly ionized atoms) and $V_a$ is the accelerating voltage. Assuming only singly ionized atoms, it is clear from the above equation that the voltage required to accelerate an atom to a given velocity, (which is proportional to specific impulse) and thus the energy the atom attains at that velocity, are both directly proportional to particle mass. Therefore, the number of electron volts per ion used in accelerating each ion to a given specific impulse is directly proportional to the propellant atomic weight.

It was pointed out earlier, however, that the energy required to create an ion did not vary much for most possible propellants, usually requiring somewhere between 30 and 60 electron volts. Including losses within the sources raises this value in terms of electron volts per ion delivered to the accelerating region to a range of about 350 to 700 electron volts, of course, but the important point is that the value is not very sensitive to what propellant is used. It is clear that the energy required to accelerate an ion must be many times these values for an ion engine to be highly efficient, whatever the material used. Placing several ionic mass values in equation 2.2-1 gives representative values for the acceleration energy per ion for a number of materials covering the range of possible propellants for $I_{sp}$ = 5000 seconds. These values are shown in Table 2.2-1 along with the resultant efficiencies for an assumed ion formation energy of 500 electron volts for all propellants.

Table 2.2.1

Ion Engine Efficiency as a Function of Various Propellants

(A constant generation requirement of 500 eV/ion is assumed)

| | Atomic Weight | Accel Energy (eV) | Engine Efficiency (%) |
|---|---|---|---|
| H | 1 | 12.5 | 2.4 |
| Ne | 20 | 250 | 33 |
| Cs | 133 | 1660 | 77 |
| Hg | 201 | 2500 | 83 |

Since the energy of ion formation of 500 electron volts per ion (at reasonable propellant utilization) is representative of current ion source requirements, Table 2.2.1 demonstrates that high atomic weight propellants are desirable for an engine based on current technology operating at $I_{sp}$ = 5000 seconds. Furthermore, it is seen that atomic weights greater than one hundred are a literal necessity to achieve even minimally acceptable efficiencies.

Taking into account the atomic weight as well as the other necessary chemical and physical properties mentioned previously restricts us to a very few materials about which sufficient ionization information is available to warrant their consideration as potential propellants. Of these the most practical appear to be mercury and cesium. In terms of engine performance, mercury has the advantage of higher atomic weight, and is compatible with the efficient barium film and barium

oxide cathodes. Cesium, on the other hand, has a lower ionization potential. This factor normally would allow a greater flexibility in source design without exceeding sputtering threshold voltages, but it is largely offset by an extremely high excitation cross section. As a result, the design flexibility of cesium and mercury sources are roughly comparable. Like mercury, cesium can also be used with efficient cathodes, since it is compatible with the tungsten-oxygen-cesium variety which are nearly as efficient as the barium types. While the W-O-Cs cathodes can be operated in equilibrium with the cesium vapor pressures existing in low density ion sources, some method of supplying oxygen for long term applications must be devised, or the available current density will fall by a factor of more than one hundred as the oxygen is depleted. The barium cathodes also require a continual supply of active material, however, so the cathode problems in both cases appear comparable.

The real criterion for choice between these propellants arises when we consider them from the point of view of acceleration system life. Comparing them on the basis of equal thrust per unit area at $I_{sp}$ = 5000 seconds and equal propellant utilization, it follows that both the ion current density and the neutral atom flux for cesium are up by a factor of 1.5 over the values for mercury. Assuming a fixed ratio between source and accel electrode voltages relative to the beam potential for both cases gives the same velocity distribution for both types of ions in the regions contributing to ion formation by charge exchange. Figure 2.2.1 shows the values of the charge exchange cross sections versus ion velocity for atoms with their own ions, and in the velocity range contributing to accel electrode wear (between 5 and 10 x $10^6$ cm/sec) the cesium cross section is seen to be larger than the mercury cross section by a factor of about 2.5. (Reference 6) Taking into account the current density ratio of 1.5 and the fact that cesium neutral atoms stay in the contributing region for a shorter time at equal neutral gas temperatures by virtue of their lower mass, the relative number of cesium and mercury ions formed by charge exchange can be calculated, yielding the ratio of 4.6 to 1. The damaging effects of cesium versus mercury are not quite in this ratio because the cesium ions strike with one-third less energy and cause a slightly lower damage per unit energy. These factors reduce the damage ratio to 3 to 1. Thus, mercury yields a substantial lifetime advantage. An engine operating on mercury at a given thrust per unit area will last three times as long as a similar engine operating on cesium at the same specific impulse. Since mercury is capable of source operation within the voltage limits set by sputtering considerations and yields overall efficiencies at least equal to cesium, there appears to be no argument favoring cesium over mercury.

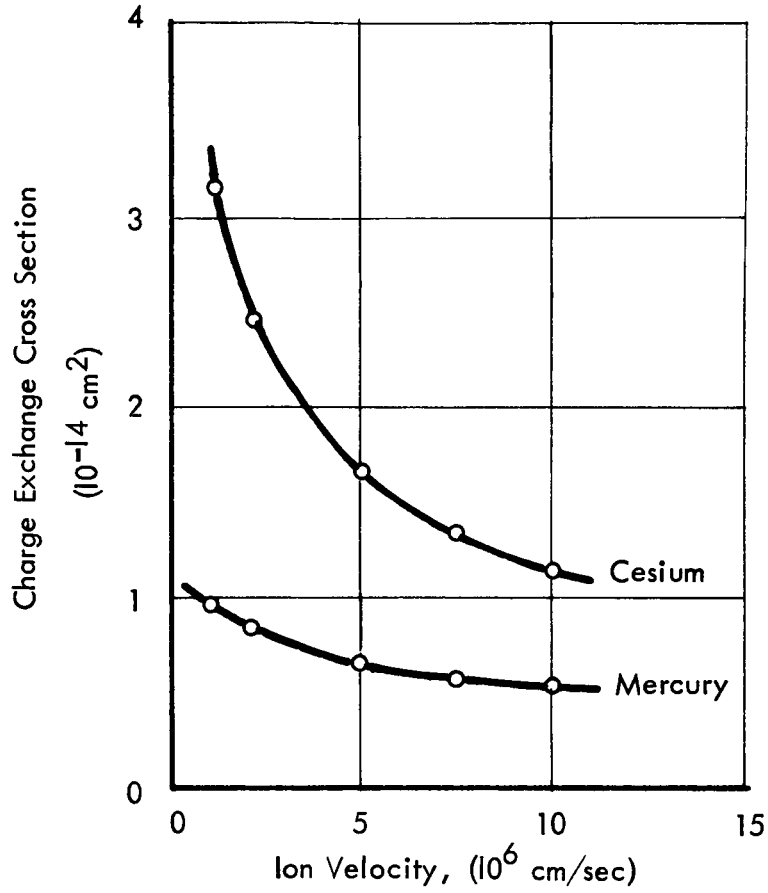


FIGURE 2.2.1

RESONANT CHARGE EXCHANGE CROSS SECTIONS VERSUS ION VELOCITY

Returning to the other methods of prolonging electrode life, it is apparent that reducing the ion current density is an effective means of decreasing the sputtering damage. Generally speaking, a decrease in current density implies an increase in engine scale, if optimum operating conditions are to be maintained. Thus, not only will ion current and neutral atom densities be decreased, but the size of the electrodes will be increased. As a result, they will be capable of undergoing more sputtering before exhibiting serious impairment in their beam forming abilities.

Control over current density without a power efficiency penalty is, of course, one of the attractive features of bombardment engines. Unlike the cesium contact ionization engines, bombardment engines can be constructed with virtually any current density desired at good efficiency. The competition between design parameters in bombardment engines is strictly one of lifetime versus average current density and is much less crucial in determining the practicality of an engine than the matter of efficiency.

The preceding extraction system discussion described the basic problems to be solved in constructing accelerator electrodes. The initial experimental work performed to study the extraction system problem was to construct an electrode system which would provide sufficient focusing of the ion beam.

The extraction geometry chosen was a modification of the well-known Pierce geometry for the space charge flow of a parallel beam from a slit source. Departures from the ideal Pierce geometry were necessary in the actual electrode design due to the physical requirements in constructing the electrodes.

The choice of the extraction geometry parameters was guided to a first approximation by three equations: (MKS units)

$$V_a = 4.06 \times 10^5 \; j/K_o^{\;2/3} \; X_o^{\;4/3} \qquad (2.2\text{-}2)$$

$$j = N_+ e \; E_A/M^{\;1/2} \qquad (2.2\text{-}3)$$

$$Y/Y_o = 1 + 2.99 \times 10^6 \; jX^2/V_a^{\;3/2} \qquad (2.2\text{-}4)$$

where $V_a$ is the minimum potential for extracting the mercury ion current density, j, $X_o$ is the acceleration distance, $K_o$ is a correction factor which is equal to 1 for the idealized Pierce geometry, but is less than 1 for other geometries, $N_+$ is the ion density of the plasma just inside the meniscus, e is the electronic charge,

$E_A$ is the average electron energy in the plasma, M is the mass of the mercury atom, Y is the width of the ion beam which is initially $Y_o$, and X is the position at which the beam width is Y. Equation (2.2-2) is Child's law modified by the factor $K_o$. Since $K_o \leq 1$, it is implied that the extraction efficiency for a specific realistic geometry is less than for the idealized Pierce geometry. Equation (2.2-3) is a statement of the maximum ion current density which can be extracted from the plasma through the meniscus. This maximum current density depends on the plasma ion density and the average electron energy inside the plasma. Equation (2.2-4) is a statement of the ion beam blow up in the drift region between the acceleration electrodes. If it is assumed that the maximum current density as given by Equation (2.2-3) is to be extracted, then Equation (2.2-2) implies that for low values of extraction potential, the acceleration distance should be small. However, according to Equation (2.2-4), a small acceleration potential difference results in a rapid beam blow up which in turn requires that the length of the acceleration electrode be small if the deceleration electrode is to be able to refocus the beam. For a short acceleration region, however, the sputtering rate due to charge exchange may be excessive.

The Pierce type electrode design was used to determine the shape of the electrodes constructed for the initial testing. Because of its low sputtering ratio, carbon was chosen as the electrode material. Optimum voltage and spacing conditions could be determined most efficiently if movable electrodes were present so a movable accel-decel extraction system was designed and fabricated. The linkage which previously had been used for probe measurements was converted to the movable electrode application. A profile view of the movable electrode assembly is shown in Figure 2.2.2. In the figure, the outer electrode rings are moved by the linkage at the top while the inner electrode rings are moved by the linkage which passes through the center of the ion engine.

The movable electrode assembly was fabricated and tests were made on the calibration and mechanical performance of it. A few minor modifications were made and then an experimental ion engine extraction test program was begun. The initial test was to be made with a mercury propellant. Some problems were encountered in getting the initial investigations of the extraction system underway, specifically insulator breakdown and outgassing of the carbon electrodes. The insulator breakdown problem was caused by ion bombardment and by deposition of sputtered material on the ceramic insulators. A shielding arrangement was designed, fabricated and installed around each insulator; the shields were two small concentric stainless

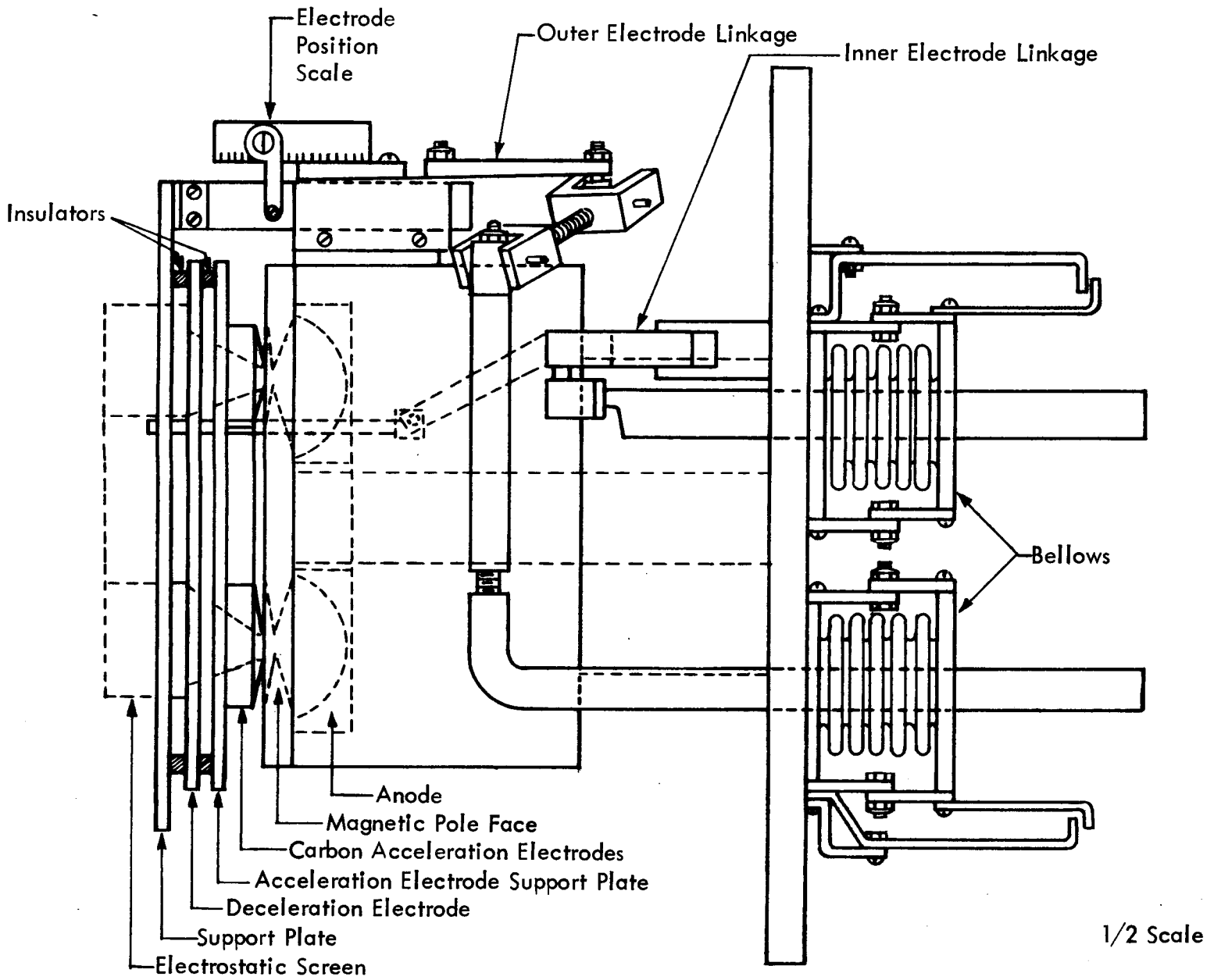


FIGURE 2.2.2 MOVABLE EXTRACTION SYSTEM DETAIL

steel cans which surrounded an insulator and prevented the deposition of sputtered material and also prevented ions from impinging on the ceramic surface. The outgassing problem was eliminated in the experiment by a change to stainless steel electrodes.

A temporary change was made to argon propellant to facilitate the initial experimentation. The basic extraction electrode design used in both the argon and mercury testing is shown in Figure 2.2.3. Tests were made on the extraction system for various accelerator electrode spacings and voltages. Figure 2.2.4 is a plot of the data to show the variation of ion interception percentage on the acceleration electrode as a function of the acceleration voltage using argon propellant and an acceleration distance of 3.5 mm. Fairly good focusing of the ion beam was obtained at acceleration voltages of minus 9 kv. However, higher negative voltages were not tried due to corona discharge. In taking the data for Figure 2.2.4, it was found necessary to lower the performance of the source to approximately 45 per cent propellant utilization at 400 eV/ion arc efficiency in order to reach even the 9 kv level. (This source performance was obtained by lowering the internal magnetic field from 200 gauss to 70 gauss.) The pressure of the vacuum system was low enough to allow extraction potentials to be applied when no ionization was being generated by the ion source; once the arc was turned on a significant corona discharge problem was encountered at extraction potentials exceeding 5 kv except when the source performance was lowered. The corona discharge resulted from the high ionization level present in the vacuum chamber when high performance operation was attempted. A discharge was easily started between the negative potential calorimeter and ground when many ions were bombarding the calorimeter.

Additional tests were made to investigate the extraction system performance with a mercury propellant. Data was taken (mercury propellant) for various extraction spacings and the performance was similar to the argon operation as was expected. The results of the test data are shown in Figure 2.2.5 where the percent of ion beam intercepting the acceleration electrode is shown as a function of the acceleration voltage for the various extraction spacings. It was found in the range of voltages tested that the smaller electrode spacings gave a smaller interception on the acceleration electrode. The curves are incomplete in that the tests of the extraction system behavior in the accel voltage region above 10 kv were not possible because of the corona discharge and the overtaxed acceleration electrode power supply. These limitations on the progress of the extraction system experiments were considered in detail, and it was decided that a major change in the engine and the experimental configuration was in order.

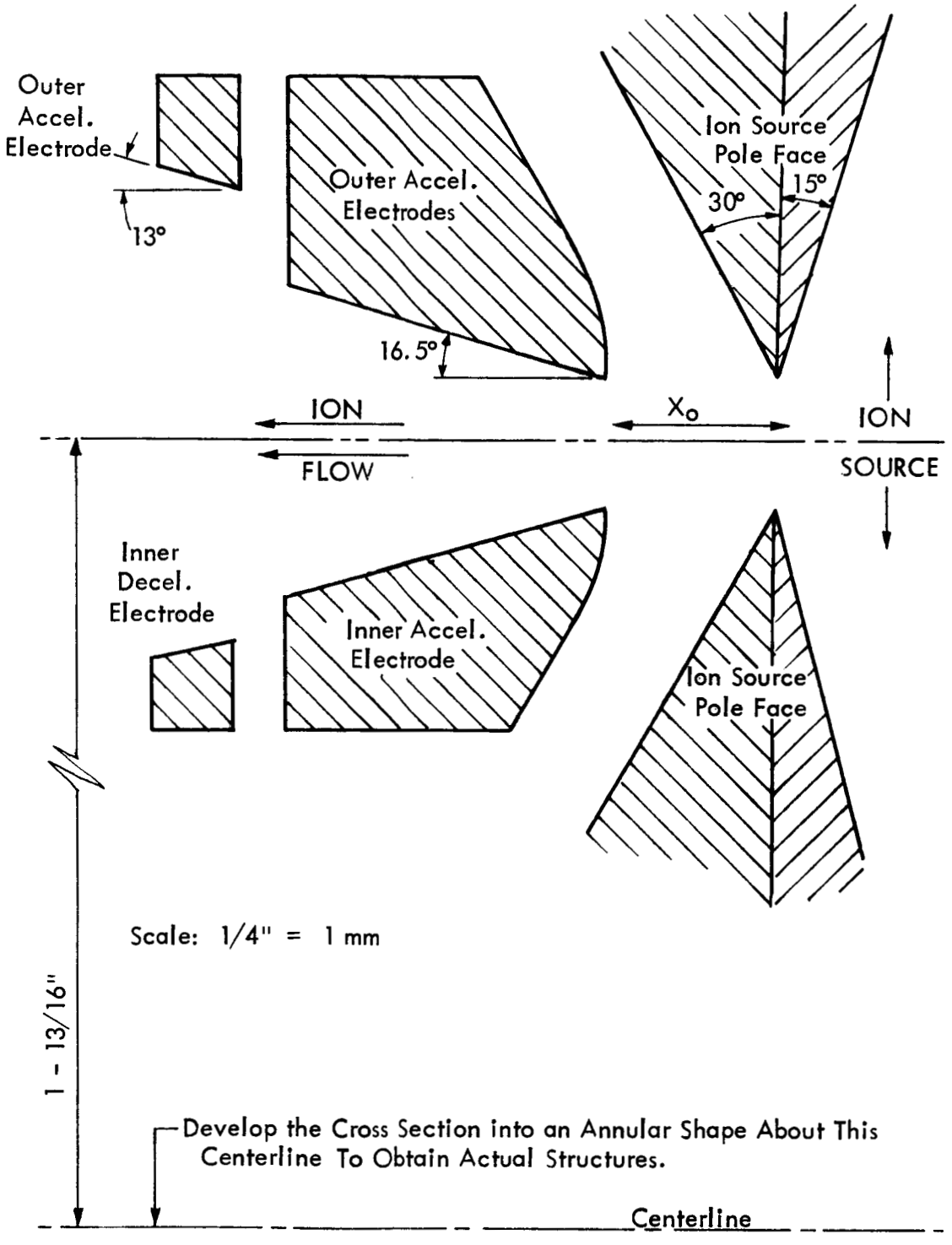


FIGURE 2.2.3 GEOMETRY OF EXTRACTION SYSTEM

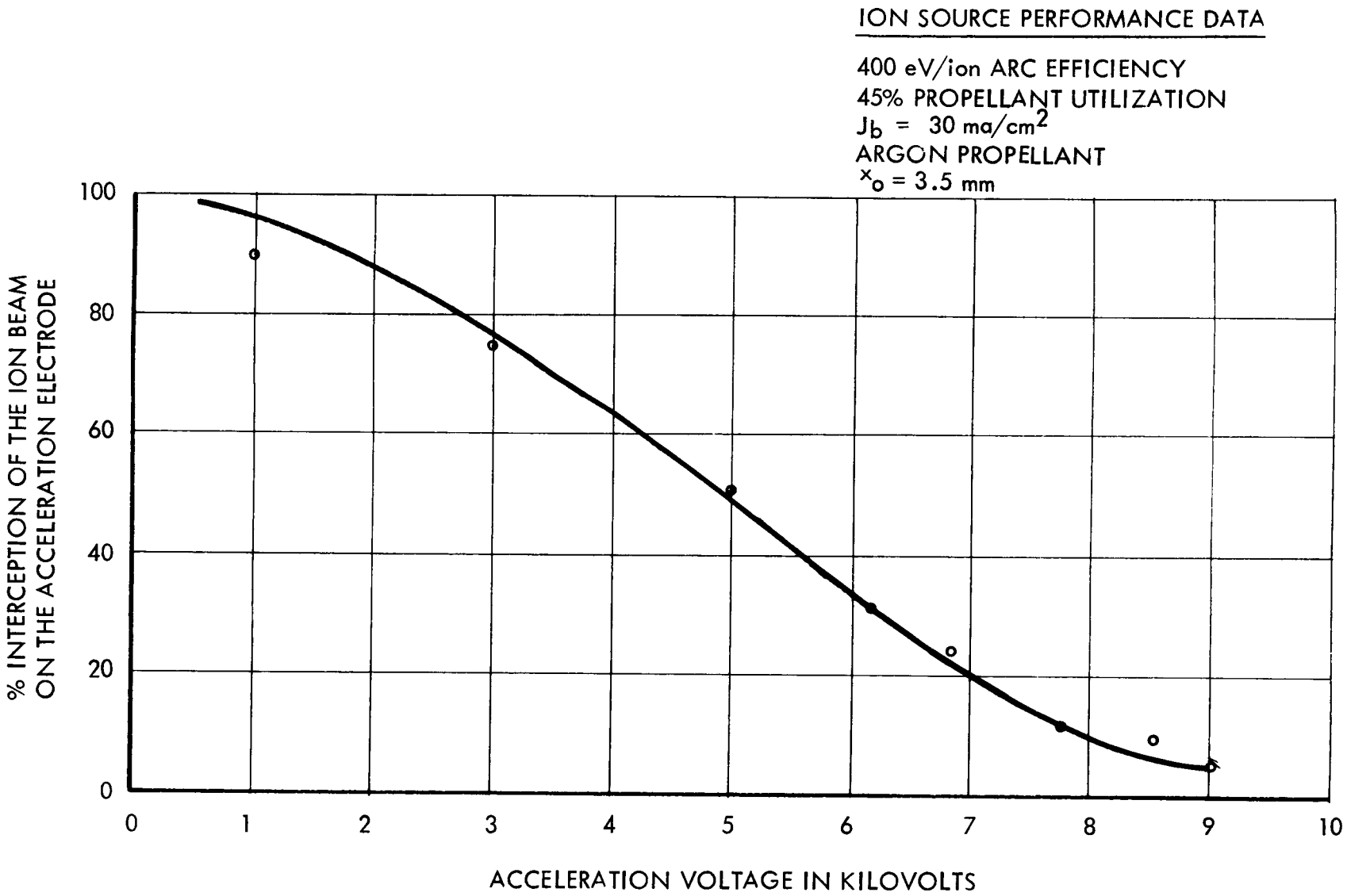


FIGURE 2.2.4 INITIAL ACCELERATION ELECTRODE INTERCEPTION DATA

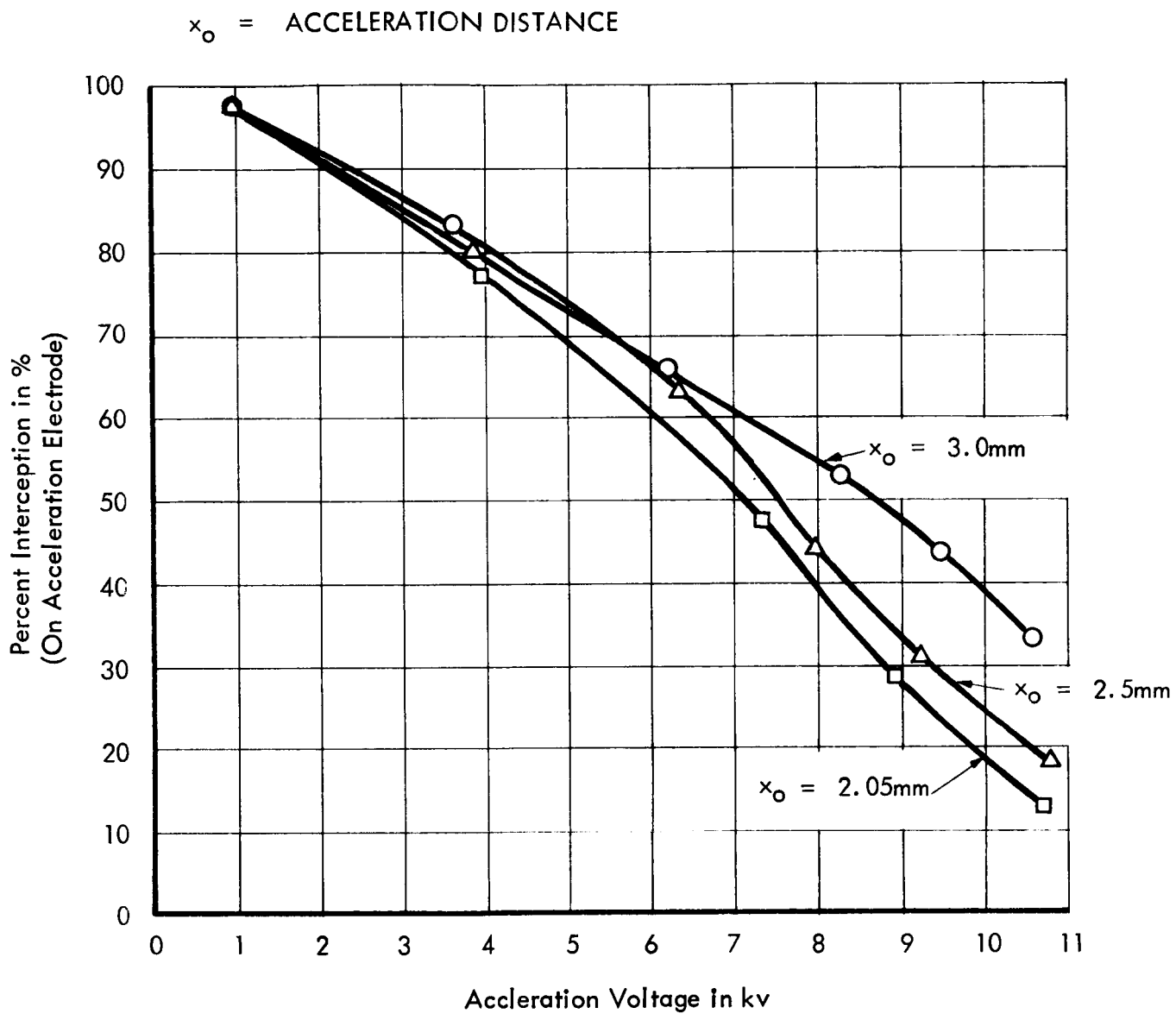


FIGURE 2.2.5 VARIABLE ACCELERATION DISTANCE ELECTRODE INTERCEPTION PERFORMANCE DATA

### 2.2.1 Four-Inch Diameter Ion Source

The course chosen was to fabricate a new engine shown in the artist's drawing of Figure 2.2.6. This engine was smaller in diameter than the eariler model and had a nominal ion beam current rating of 250-300 ma. The overall diameter of the source was four inches. All of the obsolete appendages which had been added to the earlier seven-inch diameter engine were removed and all the improvements and modifications suggested by previous experience were incorporated. Either permanent or electromagnets could be used by substitution of different back plates. Furthermore, the extraction system retained its capability of movement under operation and was firmly supported. Also, this engine was arranged for mounting at high potential.

The four-inch diameter ion source was constructed and assembled. Pictorials 2.2.1, 2.2.2 and 2.2.3 show various views of the completed ion source. Pictorial 2.2.4 shows the experimental set up. A special calorimeter arrangement was constructed to prevent the ion beam from impinging on the walls of the vacuum chamber and causing outgassing. The calorimeter was constructed with a water cooled target surrounded by a liquid nitrogen cooled coil. The water cooled target absorbed the primary ion beam power while the liquid nitrogen cooled coil provided a pumping action to rapidly remove neutral mercury atoms from the region. Performance tests of the new configuration were made and data was obtained as shown in Table 2.2.2.

A failure in the inner electrode mounting insulator in Run 4 caused the inner acceleration electrode to move slightly out of position with a high resultant interception. Because of this difficulty, it was not possible to obtain meaningful extraction system performance information in this test. Sufficient information, however, was obtained from the experiment to allow proceeding to the next phase of development of the ion source.

The performance testing of the four-inch diameter ion source was rewarding in that it had illustrated the capability of the transverse field ion source using mercury to operate with high propellant utilization at a reasonable arc efficiency and under typical extraction electric fields. The conversion from the old seven-inch ion source to the four-inch diameter ion source required a shortening of the magnetic pole faces. This was a parametric variation which previously had not been investigated although from theoretical considerations it should not be an important parameter within the limits of the conversion. The excellent performance of the four-inch diameter ion source indicated that this theoretical prediction was correct. This was an important consideration when the construction of a smaller ion engine model became desirable.

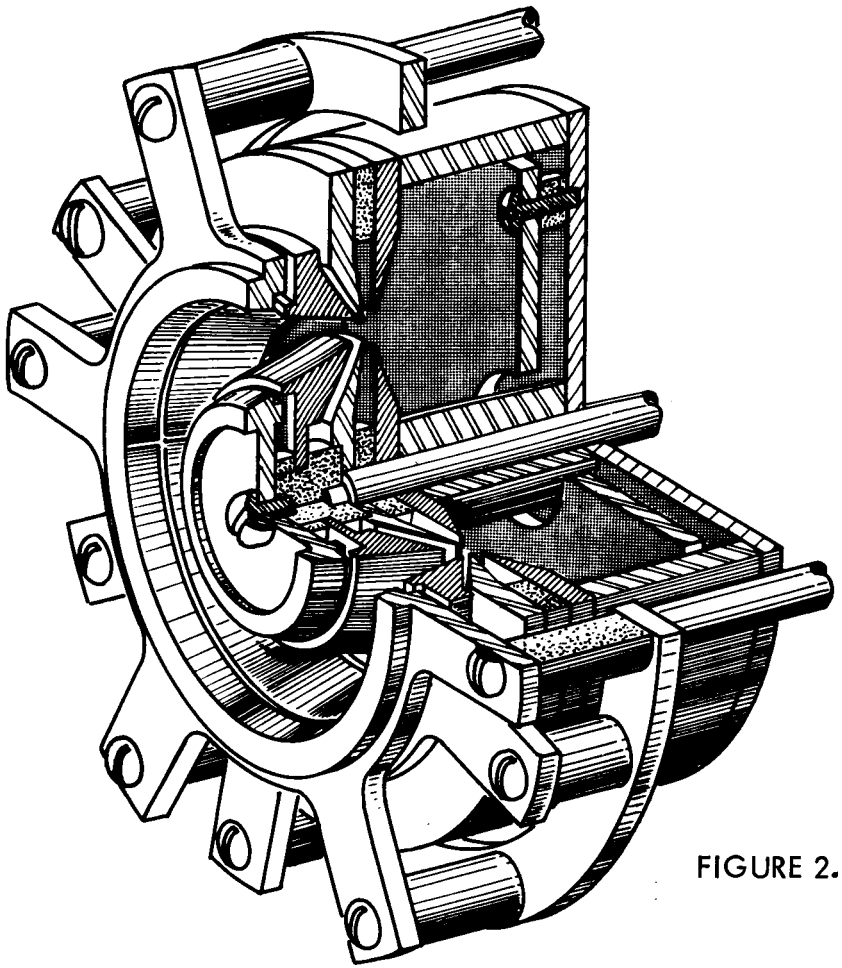

FIGURE 2.2.6 FOUR-INCH DIAMETER TRANSVERSE FIELD ION SOURCE

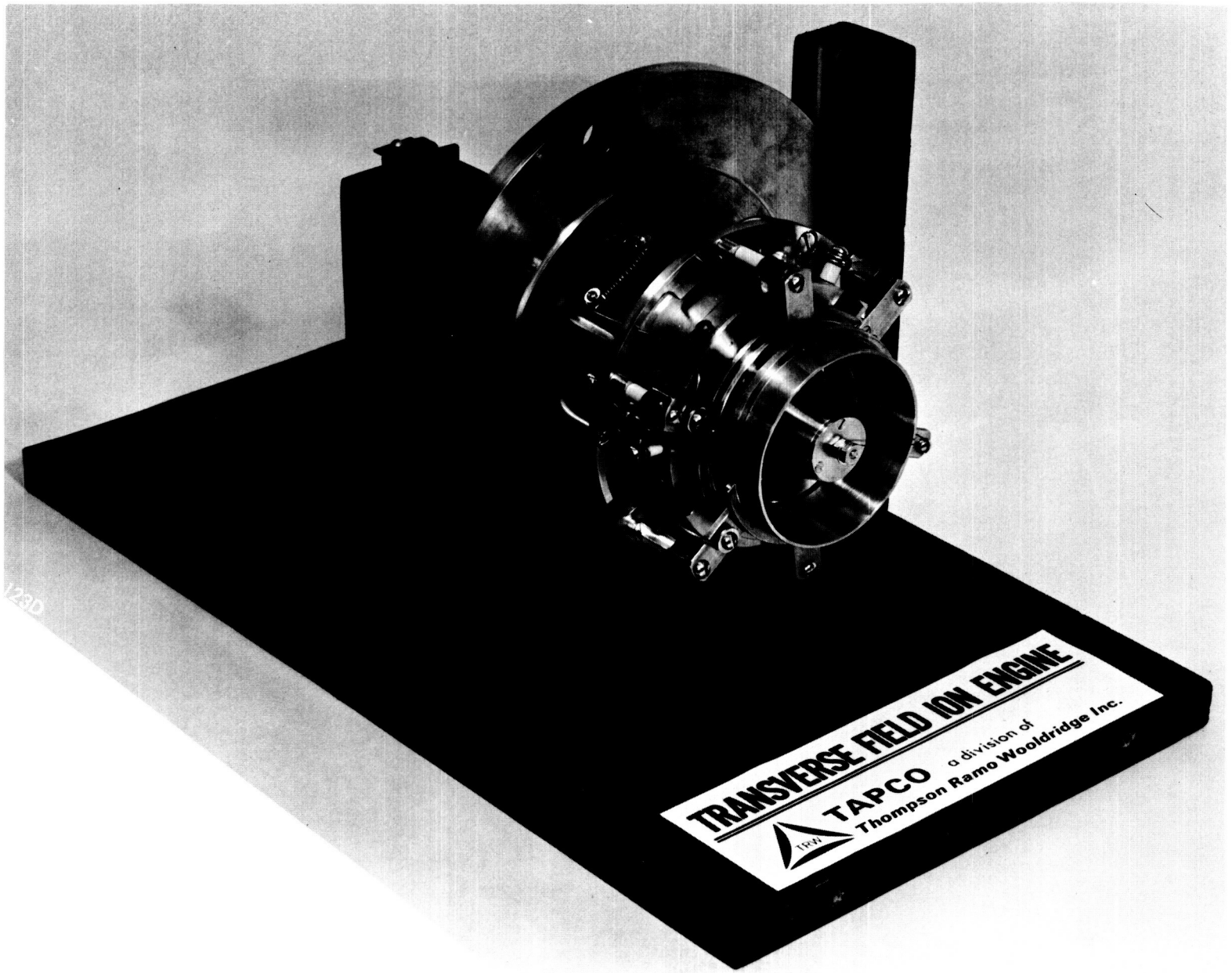


PICTORIAL 2.2.1
FOUR-INCH ION ENGINE (3/4 VIEW)

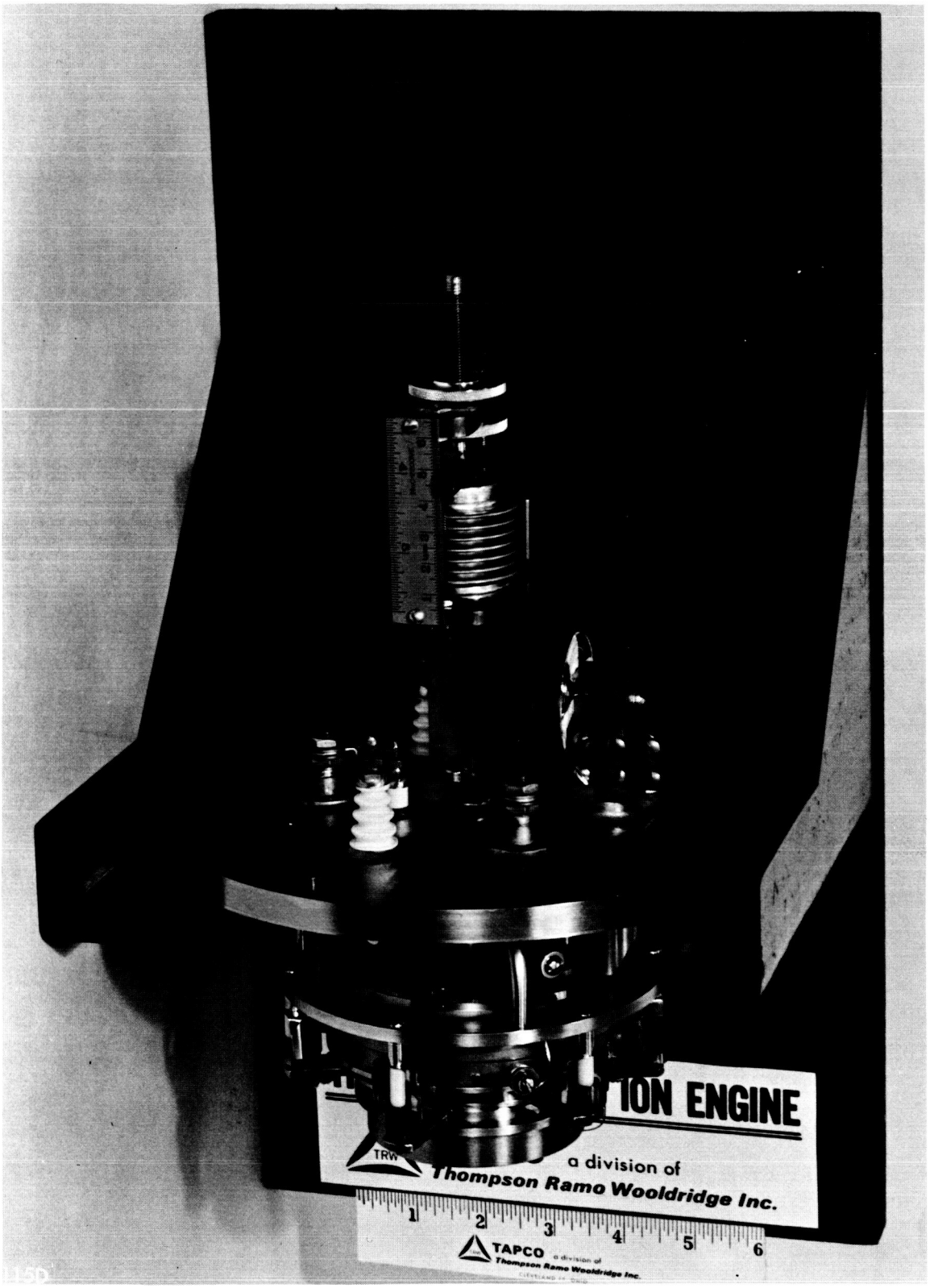


PICTORIAL 2.2.2
FOUR-INCH ION ENGINE (TOP VIEW)

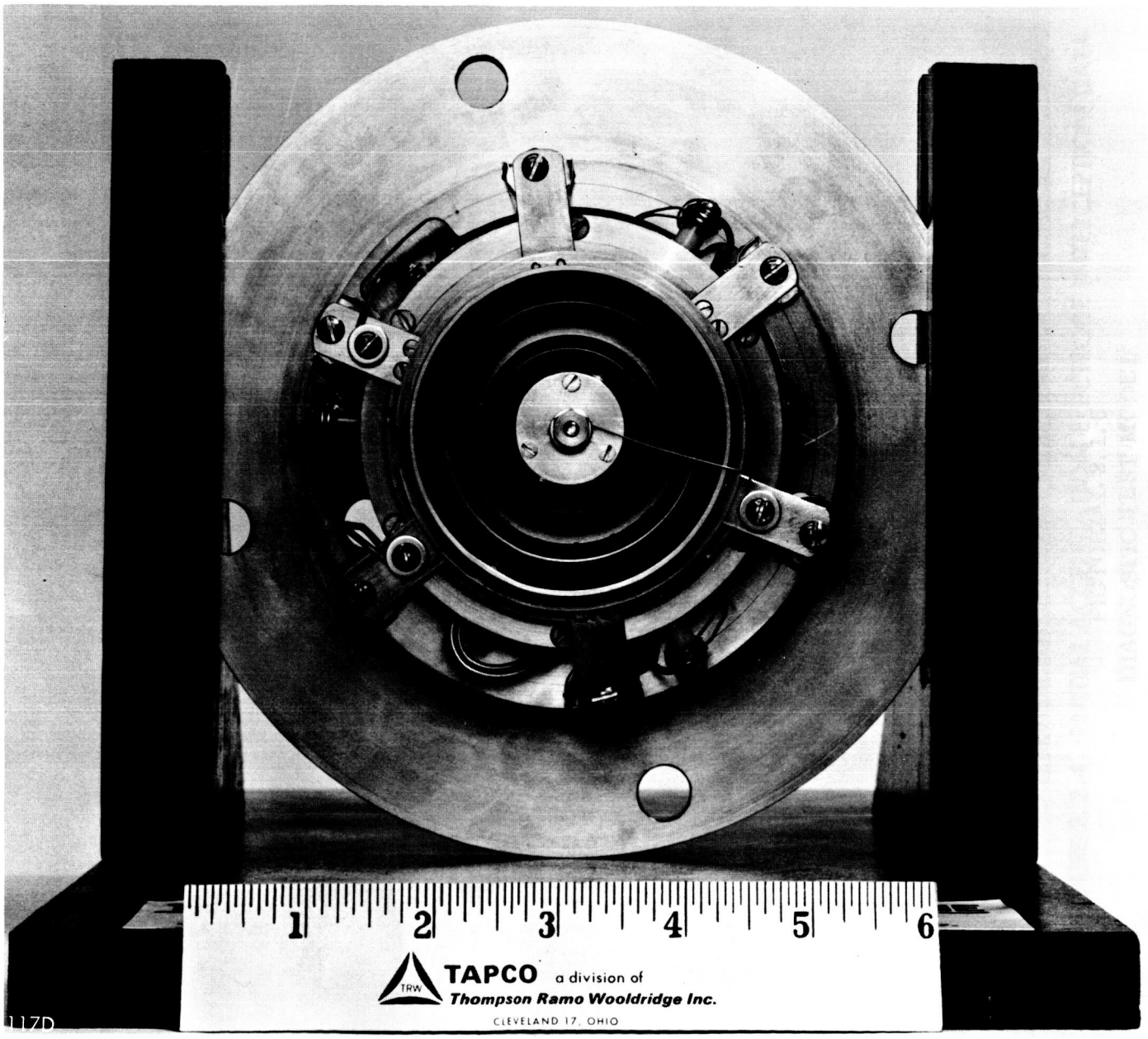


PICTORIAL 2.2.3
FOUR-INCH ION ENGINE (FRONT VIEW)

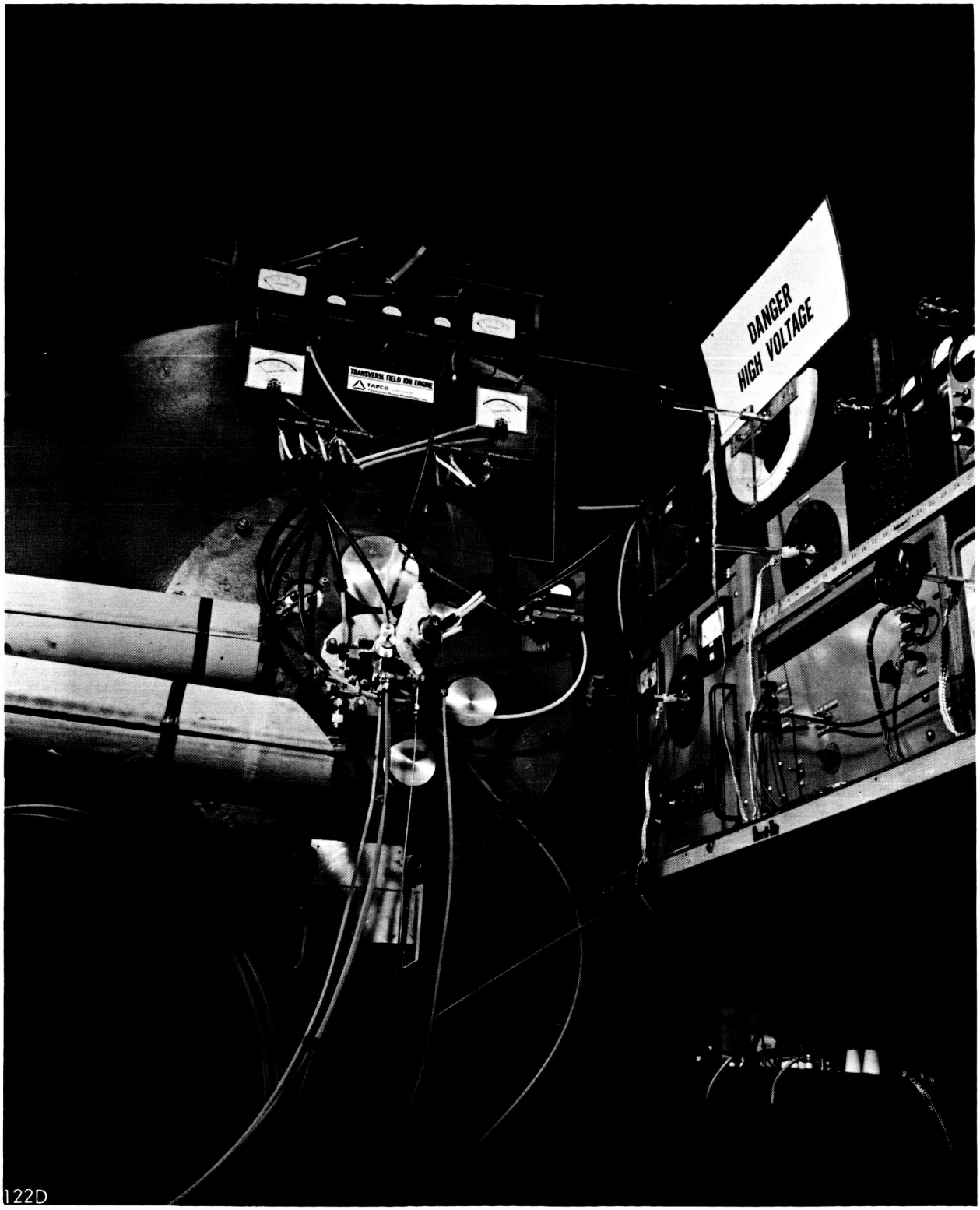


PICTORIAL 2.2.4
EXPERIMENTAL FACILITY

Table 2.2.2

Four-Inch Diameter Transverse Field Ion Engine

Performance Data

| | Run No. 1 | Run No. 2* | Run No. 3 | Run No. 4 |
|---|---|---|---|---|
| Ion Beam Current, ma | 150 | 200 | 220 | 270 |
| Source Potential, kv | +2.4 | +2.5 | +2.5 | +2.5 |
| Accel Potential, kv | -12 | -12 | -12 | -16 |
| Accel Interception Current, ma | 35 | 35 | 36 | 110** |
| Arc Voltage, volts | 30 | 28 | 37 | 55 |
| Arc Current, amps | 0.9 | 1.2 | 0.9 | 1.2 |
| Magnetic Field, gauss | 120 | 140 | 140 | 140 |
| Arc Inefficiency, eV/ion | 180 | 168 | 151 | 244 |
| Total Source Inefficiency, eV/ion | 1050 | 818 | 743 | 1274 |
| Propellant Utilization, % | 50 | 66 | 73 | 98 |
| Accel Interception, % | 23 | 17.5 | 16 | 40.7 |
| Hg Feed Rate, ma equivalent , ma | 302 | 302 | 302 | 275 |

* Higher cathode power was used on this run. The arc voltage decreases with increasing electron emission at a small cost in arc inefficiency and in cathode power.

** Broken inner accel insulator occurred on Run No. 4.

Note: 1. The cathode consisted of two twisted 0.005 inch tungsten wires (cathode power was approximately 130 watts).

2. The acceleration electrode spacing was 2.0 mm.

### 2.2.2 Two-Inch Diameter Ion Source (Mercury Propellant)

At this point in the research program, it seemed appropriate to begin serious investigations into the problem of installing a nickel matrix dispenser cathode in the ion source as well as to continue extraction electrode studies associated with the annular geometry. It was decided that the cathode studies could be conducted most efficiently if the ion source were set up in a vacuum system which would enable good visual observation of the ion source operation. The extraction electrode studies on the four-inch diameter source indicated that ion extraction from a 4 mm slit might prove difficult and it would be desirable to change the exit aperture width from 4 mm to 2 mm. Furthermore, the extraction work being performed under Contract NAS3-2522 was done with a 2 mm exit aperture, so a corresponding aperture size should be used to most efficiently utilize the information obtained from this work. All indications, therefore, were that a 2 mm exit aperture should be used to most efficiently utilize the information obtained from this work. All indications, therefore, were that a 2 mm exit aperture should used to obtain optimal extraction performance. However, modification of the four-inch diameter source to a smaller aperture was not believed to be the direction in which to proceed. An analysis was made of the relationship between the obtainable ion beam current and the frontal area size of the ion engine. For example, for a current density of 50 ma/cm$^2$ and a four-millimeter exit aperture, the four-inch diameter ion engine had a basic frontal area of 104.2 cm$^2$ and an output ion current of 300 ma giving an ion output current per unit frontal area of 2.88 ma/cm$^2$. If the exit aperture size were decreased to two millimeters, the ion current per unit frontal area would be halved, if the current density remained at 50 ma/cm$^2$. If a two-inch diameter engine were constructed, more efficient use of the frontal area could be made by reducing the width of the front pole pieces. For example, for a current density of 50 ma/cm$^2$ and a two-millimeter exit aperture, a two-inch diameter ion engine would have a basic frontal area of 26 cm$^2$ and an output ion current of 100 ma, giving an ion output current per unit frontal area of 3.84 ma/cm$^2$, considerably higher than even the original four-inch diameter ion engine with a four-millimeter exit aperture. The fact that the exit aperture width should be decreased to two millimeters and the basic geometric superiority of the smaller ion source diameter indicated that the most efficient and rewarding experimental effort would be to build a smaller ion source.

Sufficient benefit could be derived to warrant the construction of a smaller ion source model so a two-inch diameter ion source configuration with a 100 ma ion beam design current output was planned: the two inch size was believed to be the proper compromise between maximum current per unit frontal area and fabrication difficulty with small size components.

The design of the two-inch diameter ion source model was essentially a scaled down version of the four-inch diameter model. This two-inch diameter model was constructed and was mounted on the same mounting configuration as had been used for the four-inch diameter model. Pictorial 2.2.5 shows the completed assembly of the two-inch diameter model.

The test program for evaluating the performance of the two-inch diameter ion source was begun and the initial testing revealed a problem in achieving a satisfactory mounting arrangement for the inner acceleration electrode. The small size of the ion source made a conventional insulator mounting technique difficult. It was decided that the best way to solve the problem was to eliminate the inner acceleration electrode insulator to the outer acceleration electrode. This technique required bridging the ion beam with support wires. An interception problem of mercury ions striking the support wires would exist unless a shielding arrangement were provided. This shielding arrangement was accomplished by placing small tabs across the exit aperture of the ion source directly beneath the inner accel electrode support wires. An additional benefit was derived from the shielding tabs placed across the exit aperture, in that the cathode to anode region beneath the tabs was shielded from the extraction potential. It was possible to start the arc while the full extraction potential was present. The arc then spread immediately to the rest of the arc chamber around the annulus and an acceptable start up procedure was obtained. This ability to start the ion engine while the full extraction voltage is applied is important in minimizing extraction power supply weight and in minimizing start up electrode erosion effects. A diagram of the shielding configuration is shown in Figure 2.2.7.

The two-inch diameter ion engine was tested and steady state ion beam extraction was accomplished at rated output ion beam currents. Typical performance values obtained are those shown in Table 2.2.3.

There are a few characteristics of the operation which are noteworthy. At a cathode temperature of 2400°C and at 90 per cent propellant utilization, the arc efficiency was approximately 360 eV/ion and the arc voltage was approximately 27 volts. The arc voltage was found to increase somewhat in the 90 to 98 per cent propellant utilization region. At 98 per cent propellant utilization the arc voltage was 36 volts. Above 98 per cent propellant utilization, the required arc voltage and eV/ion increased rapidly. It appears that a compromise between cathode lifetime (determined by arc voltage and cathode temperature) and extraction electrode lifetime (determined by propellant utilization) will result from the ion

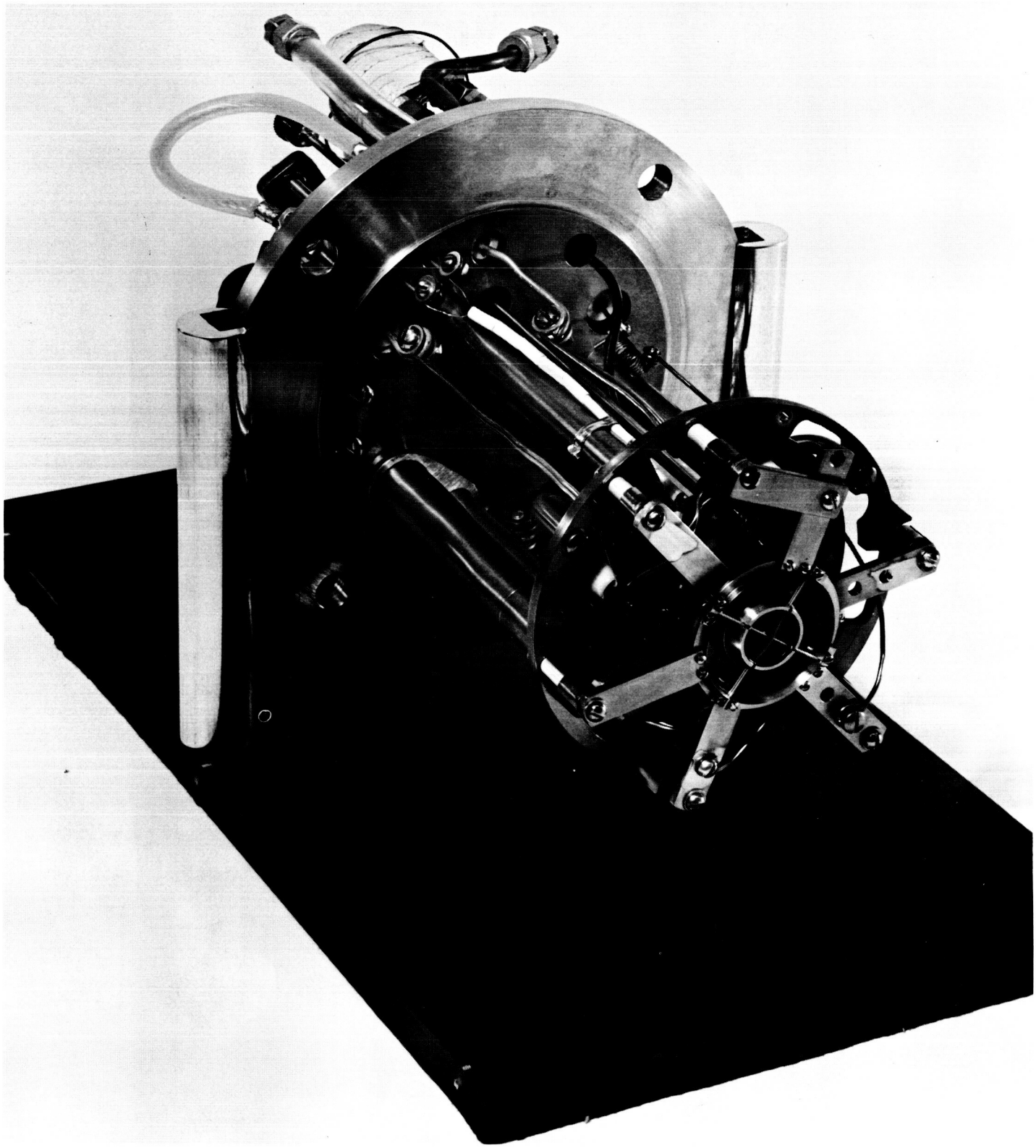

PICTORIAL 2.2.5
TWO-INCH ION ENGINE
3/4 VIEW

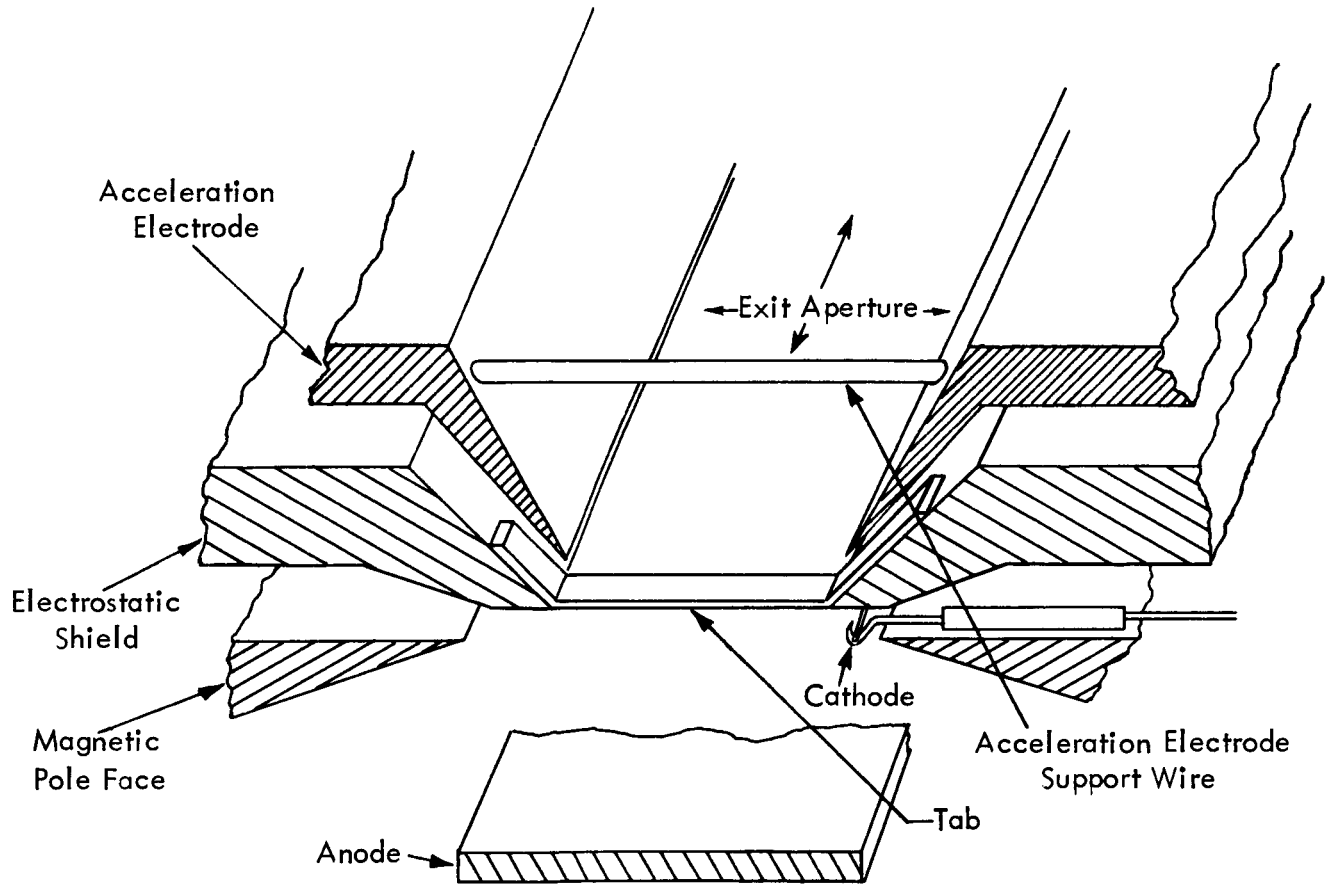


FIGURE 2.2.7 INNER ACCELERATION ELECTRODE MOUNTING ARRANGEMENT

Table 2.2.3

Performance Data of Two-Inch Diameter Ion Engine (Tungsten Cathode)

| | |
|---|---|
| Heating Power, watts | 88 |
| Magnetic Field, gauss | 140 |
| Arc Voltage, volts | 36 |
| Arc Current, amps | 1.5 |
| Source Potential, kv | +2.5 |
| Accel Potential, kv | -14.5 |
| Ion Beam Current, ma | 105 |
| Acceleration Electrode Current, ma | 12 |
| Deceleration Electrode Current, ma | 3 |
| Hg Flow Rate, ma equivalent, ma | 107 |
| Propellant Utilization, % | 98 |
| Arc Inefficiency, eV/ion | 514 |
| Total Source Inefficiency, eV/ion | 1350 |
| Engine Power Efficiency, % | 39 |

source operating characteristics. Data was taken at a high propellant utilization (98 per cent) to allow information to be obtained relative to the arc voltage vs. propellant utilization compromise. The length of the run represented by the above data was ten minutes. At this point (at 98 per cent propellant utilization) the cathode power was increased to determine if the arc voltage could be lowered by increased electron emission. The arc voltage was lowered from 36 volts to 25 volts before a cathode burn out occurred.

Immediately after the test was terminated, the propellant supply was calibrated by measuring the rate of mercury flow as a function of time. This data indicated that the propellant supply was functioning properly and that the per cent utilization number was correct to within four per cent (standard deviation of data points). Room temperature changes during the experiment were not accounted for and this represents an additional possible error in the mercury flow for this experiment. To reduce the possible error from room temperature changes, a water bath was constructed for the mercury supply line for use in subsequent testing.

Another milestone, the achievement of an efficient extraction system, had also been reached. It was not the purpose of the research to go further into the development of extraction systems at this time since parallel work on extraction systems was being performed under Contract NAS3-2522.

### 2.3 Cathode Studies

The final major problem to be solved was the problem of furnishing the electrons to the discharge using an efficient cathode. It was decided to continue with the nickel matrix cathode research since this type of cathode seemed to hold the most promise in satisfying the electron emission requirements.

The problem of installing a nickel matrix cathode in the transverse field ion source was basically the mechanical problem of supporting a thin strip of hot nickel matrix material around the exit aperture annulus. The thin strip of nickel matrix material must be heated to temperatures of 1000°C to allow activation to occur. The heating requirement complicates the mechanical problem. The heating requirements appeared to be solvable with a directly-heated wire technique. Therefore, the original nickel matrix cathode concept was a nickel matrix wire suspended in the ion source from insulated studs and directly heated. However, this concept was not immediately satisfactory due to the fact that the sintered nickel matrix material in wire form is brittle and is difficult to fabricate and support without breaking. It was decided that a superior configuration would result if the nickel matrix material were inclosed in a metallic sheath which would provide both mechanical strength and direct heating. A pure nickel sheath was fabricated as is shown in the cross section view of Figure 2.3.1.

The cathode sheath was held in a sandwich with mica as an insulator. Nickel and emitter mix powder (79% Ni, 20% emitter mix, 1% ZrH) was pressed into the cavity using an arbor press. This cavity assembly was tested in a diode experimental set up (high mercury pressure) and a current density greater than 3 amps/cm$^2$ was obtained after activation. The cathode assembly was then placed in the ion engine, but a short circuit terminated the test before significant emission could be obtained.

An attempt was made to fabricate the cathode sheath by stamping out the desired form (Figure 2.3.1) from 0.005-inch thick foil. The mechanical characteristics obtained by this method were excellent. Unfortunately, the cross section of the sheath was too small to allow adequate heating of the nickel powder in the cavity and activation of the cathode was not possible.

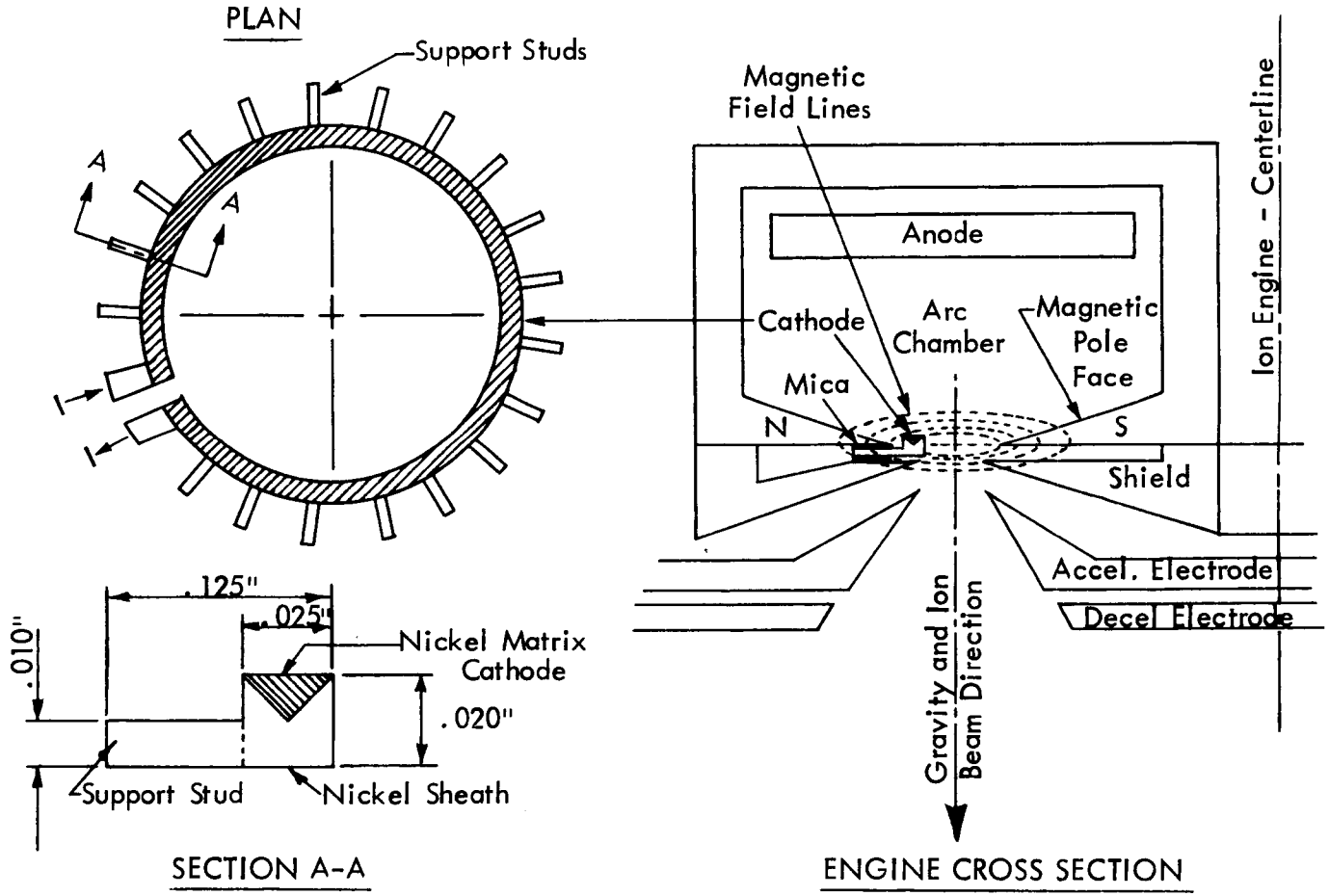


FIGURE 2.3.1 CATHODE ASSEMBLY DETAIL I

Additional cathode sheaths similar to that shown in Figure 2.3.1 were fabricated and tested. The mica insulator was replaced with Sauereisen Electrotemp Cement (No. 8 powder), a superior insulating material. The ion engine was equipped with a movable cover plate which closed off the exit aperture to allow cathode activation in the ion source under a higher discharge pressure than is ordinarily available. This cover plate eliminated the need for activation in the diode set up and allowed complete pressure control in the ion source. Tests were made with a cathode in the ion source and performance equal to that obtained previously in the diode set up was achieved in the high pressure situation. However, when the pressure was lowered by partially removing the cover plate, the discharge current decreased significantly from 2 amperes to 0.2 amperes. Also, the magnetic field had a beneficial effect on the high pressure discharge while increases in magnetic field decreased the low pressure current. It was determined from the characteristics of the operation that the high pressure cathode emission was temperature limited while the low pressure cathode emission was space charge limited. This space-charge-limited operation was not present in the transverse field ion source operation with a tungsten cathode.

The cause of the space-charge-limited operation was due to the geometrical orientation of the cathode in the magnetic field. The cathode was constructed with the emitting surface parallel to the magnetic field as shown in Figure 2.3.1. This geometry was chosen for mechanical simplicity. However, the presence of the magnetic field at the surface of the cathode caused a suppression of the electron emission. At low discharge pressures, the magnetic field retarded electron emission giving a space-charge-limited operation with a maximum arc current of 0.1 amperes, with the cover plate completely removed. At higher discharge pressures, the cathode sheath was small and temperature-limited cathode operation was obtained in spite of the magnetic field (collisions allow electron migration across the magnetic field lines). This cathode orientation concept had been originally neglected for mechanical simplicity. The obvious corrective measure was to rebuild the cathode as shown in Figure 2.3.2. Then the magnetic field will not cause suppression of the electron emission since movement of electrons along magnetic field lines is unimpeded. This new cathode was constructed and tested. There was a significant improvement in the cathode emission characteristics with several amperes of arc current available in the low pressure discharge (cover plate completely removed). A five minute run was made to obtain preliminary information on the ion engine performance. Data from this run are shown below in Table 2.3.1

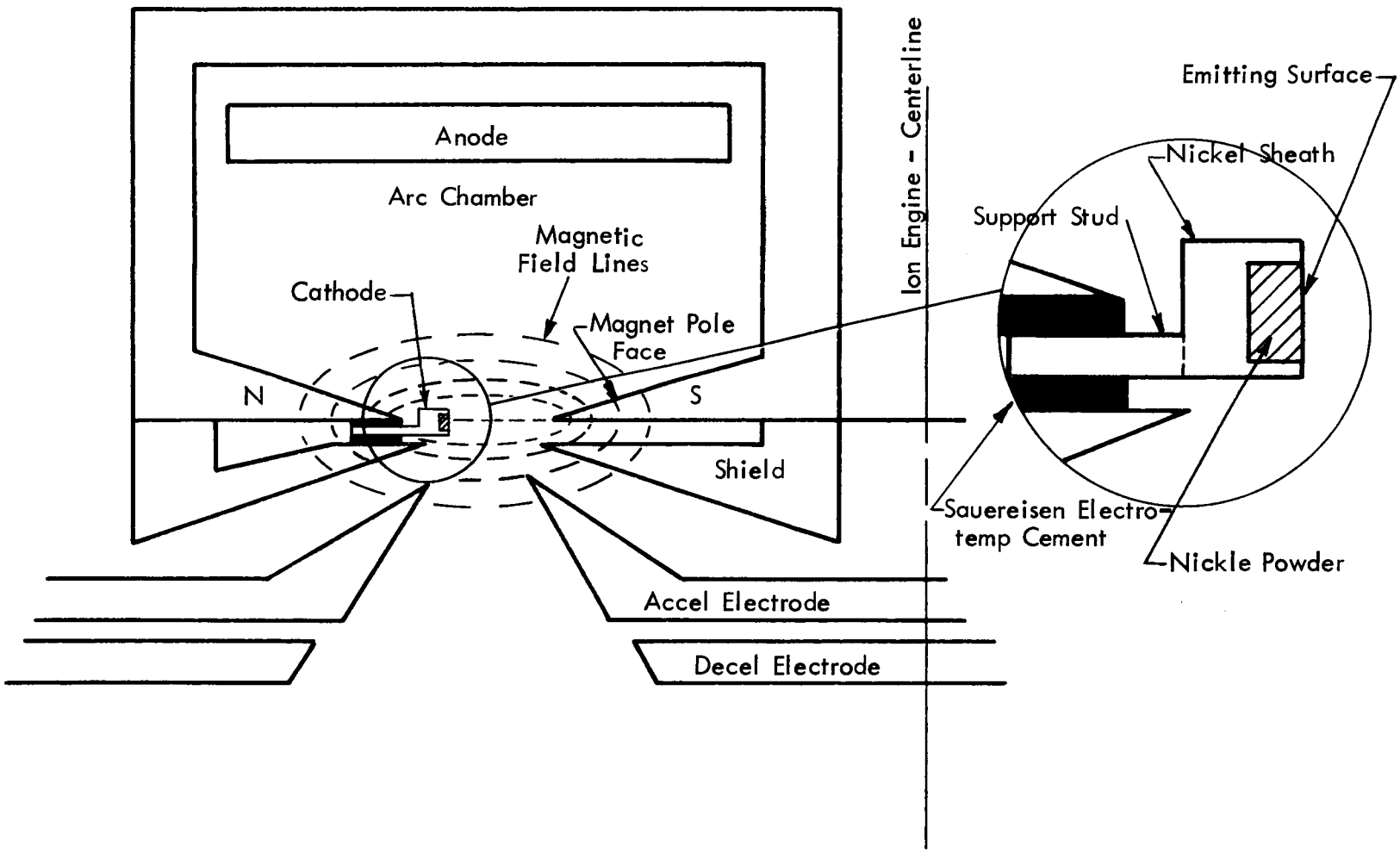


FIGURE 2.3.2 CATHODE ASSEMBLY DETAIL II

The performance data appeared very encouraging in that the operation was very similar to the operation obtained with a tungsten cathode. The arc voltage and cathode temperature were higher than desired.

Table 2.3.1

Initial Performance of Transverse Field Ion Engine with Nickel Matrix Cathode

| | |
|---|---|
| System Pressure, torr | $2 \times 10^{-5}$ |
| Cathode Temperature, °F | 2000 |
| Filament Voltage, volts | 5.3 |
| Filament Current, amps | 15 |
| Magnetic Field, gauss | 150 |
| Arc Voltage, volts | 55 |
| Arc Current, amps | 1.2 |
| Engine Potential, kv | +2.5 |
| Accel Potential, kv | -11 |
| Total Ion Beam Current, ma | 105 |
| Hg Feed Rate, ma Equivalent, ma | 114 |
| Accel Current, ma | 8 |
| Decel Current, ma | 4 |
| Accel Interception, % | 7.6 |
| Arc Inefficiency, eV/ion | 629 |
| Total Source Inefficiency, eV/ion | 1385 |
| Propellant Utilization, % | 92 |
| Engine Power Efficiency, % | 47 |

Several additional cathodes of this type were fabricated, installed, and tested. The attempt was made in all tests to locate the cathode emitting area centrally in front of the pole face point since the optimum position for the introduction of electrons to the plasma is the position where the maximum magnetic field is available. The first cathode, used to obtain the data of Table 2.3.1, had an emitting area of 0.725 $cm^2$. The second cathode tested had a larger emission area so that a larger number of electrons would be available for the crossed field discharge. The emitting area was increased to 1.0 $cm^2$. A test was made of the ion engine performance. The results of this performance run are shown in Figure 2.3.3.

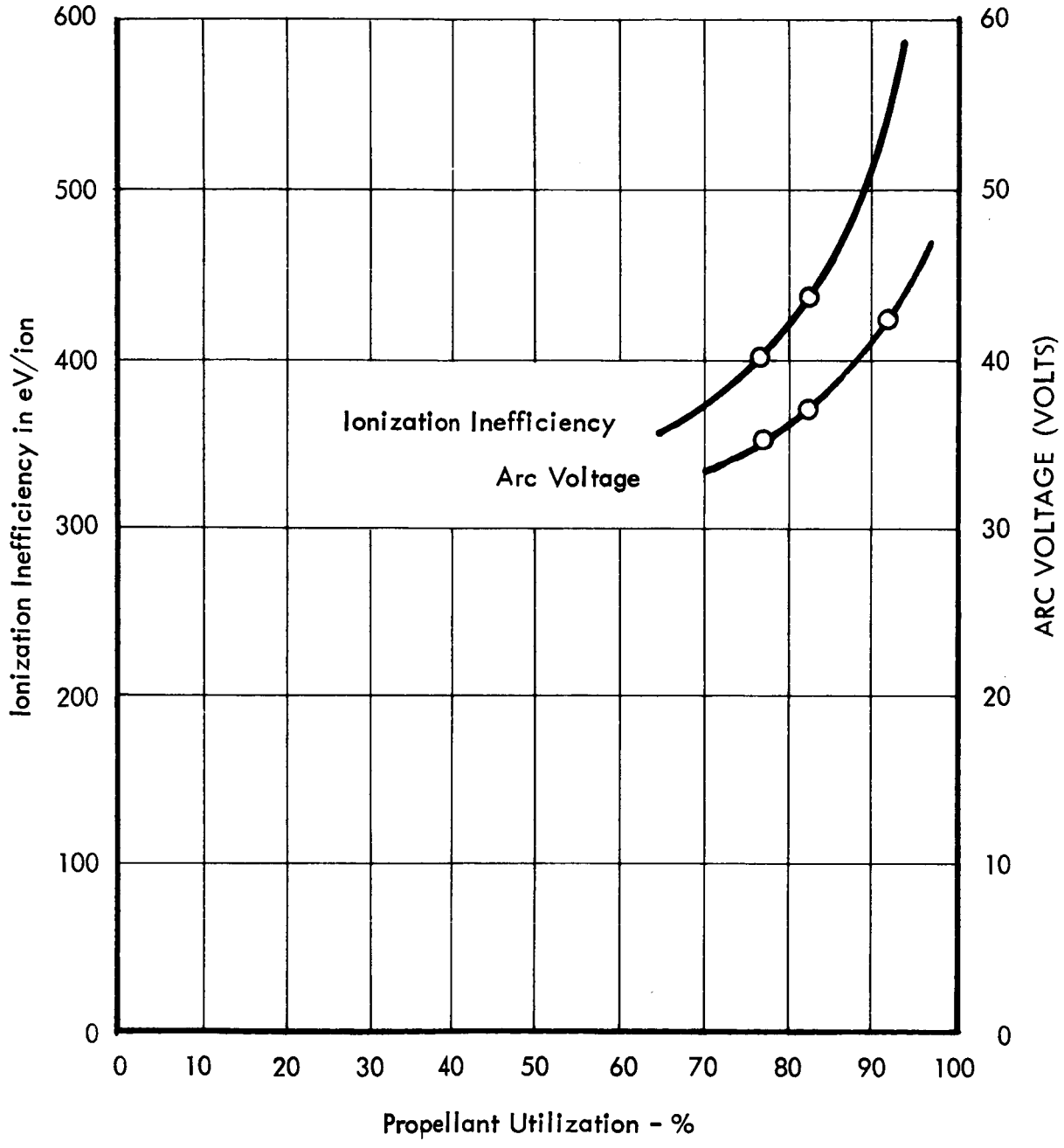


FIGURE 2.3.3. PERFORMANCE CHARACTERISTICS OF THE TWO-INCH ION ENGINE WITH A POWDERED NICKEL MATRIX CATHODE

The arc voltage had decreased to 42 volts for a propellant utilization of 92 per cent from the performance (55 volts) of the previous cathode. The increase in emitting area had a beneficial effect on the arc voltage. The total eV/ion was not improved, due to the increased heater power requirements.

An arrangement to maximize the emitting area in the allowable space was devised. The concept was to locate cathodes in front of both the inner and outer pole faces, as shown in Figure 2.3.4. Modification of the ion engine assembly was necessary to install the inner cathode.

Unfortunately, there were several basic difficulties associated with mounting cathodes on both sides of the exit aperture. These difficulties were propellant leakage behind the cathodes, difficult mechanical tolerances, and high cathode heater power consumption which overheated the magnetic pole faces. The obvious solution to these problems was to mount the cathode structure in the center of the exit aperture and have the cathode structure emitting electrons toward both the inner and outer pole faces. This configuration is shown in Figure 2.3.5. The cathode structure was fabricated from tantalum to improve the direct heating capabilities. A test was made of the ion source performance with the cathode configuration shown in Figure 2.3.5. Typical operation was in the 50 per cent propellant utilization region for arc voltages in excess of 32 volts. Several additional tests were made, but further improvements in cathode performance were not obtained.

The concept of using powdered nickel and emission mix was reexamined in the light of the experimental results. Many cathode configurations and exit aperture geometries had been tried without significant improvement in the arc voltage and current characteristics. There existed the possibility that a pressed and sintered nickel matrix cathode was a better electron source than the unpressed powder cathode. The only reason for the use of the unpressed cathode was that it was mechanically easier to fabricate and install. Installing a directly-heated pressed and sintered nickel matrix cathode wire is difficult because it is very brittle. However, it seemed advisable to attempt this difficult task and to install a pressed and sintered nickel matrix cathode.

The problems of installing a pressed and sintered nickel matrix cathode in the transverse field ion source result from the required geometry of the cathode structure and from the mechanical properties of the cathode material. The required geometric form is that of a thin ring and according to the results of Reference 7

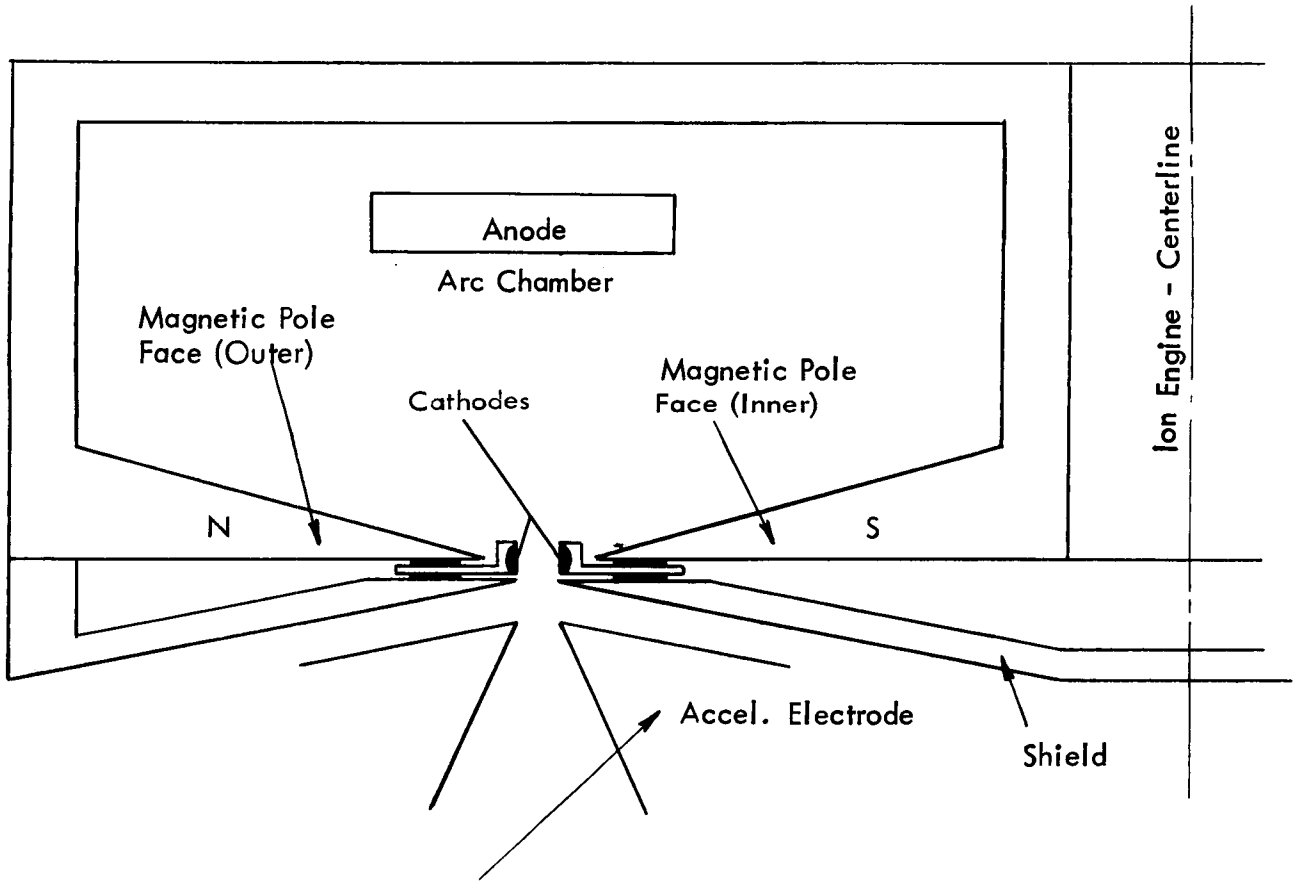


FIGURE 2.3.4 CATHODE ASSEMBLY DETAIL III

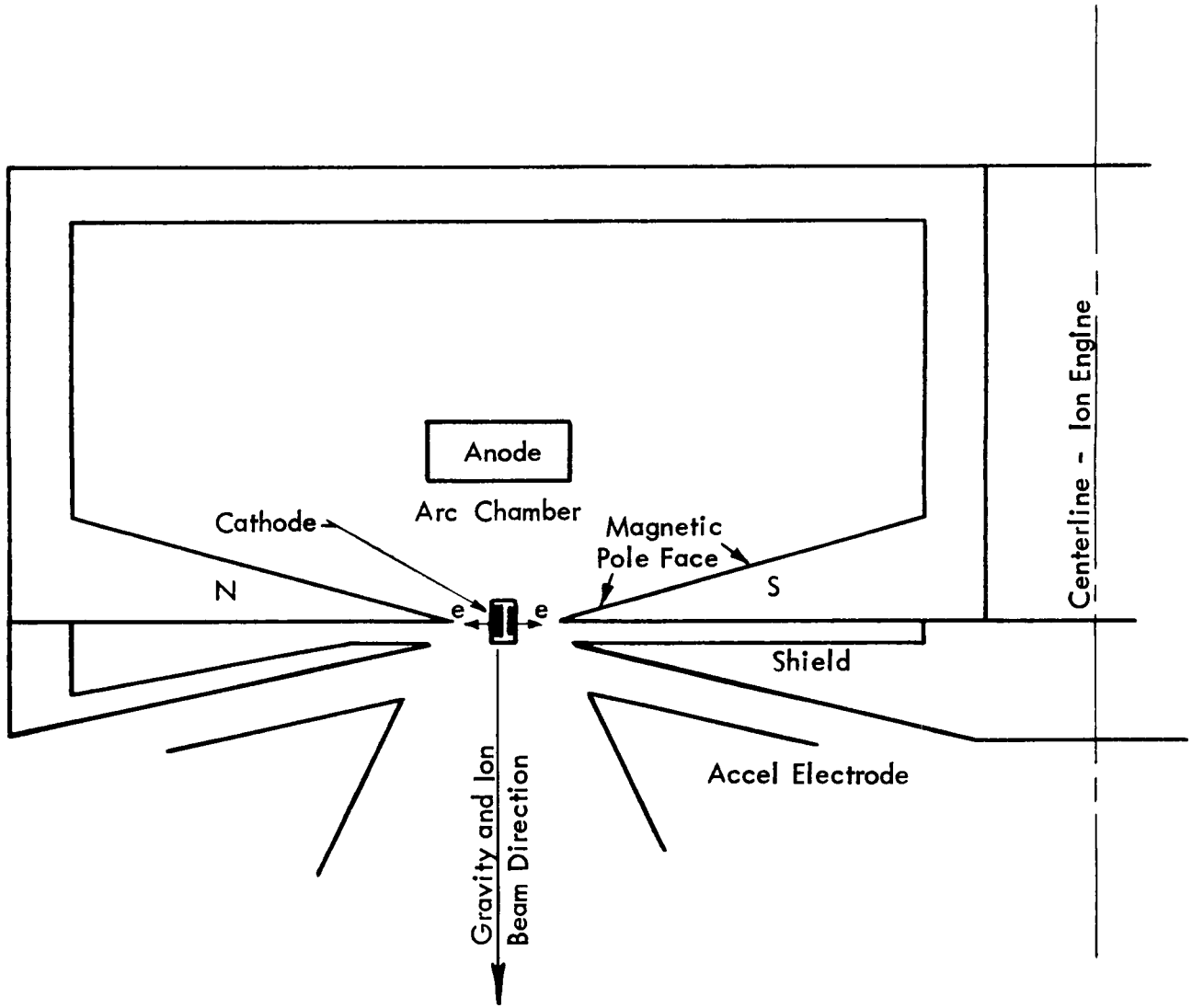


FIGURE 2.3.5 CATHODE ASSEMBLY DETAIL IV

the fragility and porosity of the sintered nickel ring will depend upon the sintering procedure. According to Reference 7, minimum sintering will result in extreme fragility and maximum porosity whereas increased sintering will yield increased strength but decreased porosity of the cathode material. A compromise between fragility and porosity must be made. In addition, sintering techniques must be such as to minimize the formation of cracks and voids which weaken or sever a thin ring. A good mounting technique must be devised which will allow the ring to be mounted without stress. Finally, if the ring is to be directly heated by electrical means a lossless, reliable electrical connection must be made.

Sintering techniques were investigated in an attempt to improve the structural properties of the cathode for the initial installation. Several tests were made in the vacuum sintering facility where the cathode material was heated by induction heating. It was found that a satisfactory absence of cracks in the stock was achieved when the vacuum system pressure was kept below 150 microns. This pressure requirement was a measure for limiting the internal pressures in the cathode stock caused by outgassing and carbonate breakdowns. The pressure requirement allowed proper adjustment of the heating rate. About sixteen hours of heating were required to bring the cathode stock to a temperature of 1000°C. The cathode stock was sintered above 1000°C for an hour and this gave satisfactory machining properties. It was also found that the probability of cracks forming in the cathode stock was decreased if the cathode stock was machined into a toroidal shape before sintering.

The installation of a pressed and sintered nickel matrix cathode was accomplished, and when tested a significant improvement in the emission characteristics was noted. The arc voltage was in the 15-25 volt range instead of the previous 30-40 volt range. In addition, when the mercury flow rate was decreased from 130 ma equivalent current to 99 ma equivalent current, the arc voltage decreased from 21 to 19 volts. These phenomena were not completely understood at this time. It is possible that other variables in the system may have been responsible for the apparent improvement in emission.

Difficulties were encountered in maintaining the electrical connections to the filament, so several methods for mounting the cathode ring were investigated. The best mounting method found was a four point support with tantalum studs. The electrical current for heating the ring was brought in one side and taken out of the opposite side of the ring; the two halves of the ring being connected in parallel. A problem of maintaining the electrical connections occurred upon

heating the ring and was solved by developing a spot welding technique to attach the tantalum studs to the nickel matrix cathode. At this point the research effort was ended due to the approaching termination date of the contract period.

## 3.0 CONCLUSIONS

The achievements of the experimental research program for investigating a transverse field ion source can be summarized as follows: The construction of a transverse field ion source was accomplished and ion source performance was investigated; an extraction system was constructed and studied; advances were made in understanding the operation of a nickel matrix cathode in a transverse field source.

It is evident from the experimental results that extremely efficient ion source performance is possible with the transverse field ion source concept (arc inefficiencies less than 200 eV/ion have been obtained above 90 per cent propellant utilization). The major problem remaining to be solved is the cathode problem. An efficient long lived cathode is necessary for a workable ion thrustor system.

There are two promising possibilities for solving the cathode problem. The first possibility is the use of a nickel matrix dispenser cathode on which a considerable amount of work has already been performed. Further work may substantiate the feasibility of the nickel matrix cathode. The second possibility for solving the cathode problem is to replace the mercury propellant with a cesium propellant and utilized the excellent emission characteristics, long lifetime, and simplicity of a cesiated tungsten cathode. Theoretical studies have been made for the operation of the cesium propellant in the transverse field ion source and the indications are that cesium would be a superior propellant in this application.

## 4.0 REFERENCES


1. Kaufman, Harold R., "The Electron-Bombardment Ion Rocket", NASA E-1862.
2. TRW Ion Engine Staff, "Summary Report on Bombardment Ion Engine Development", Final Report on Contract NAS8-42, TRW ER-5180, October 1963.
3. Bethe, H. A., and Ashkin, J., "Passage of Radiation Through Matter", Part II of Experimental Nuclear Physics, Vol. I., E. Segre', Ed., John Wiley and Sons, New York, 1953.
4. Fane, R. W., Brit. J. Appl. Phys., 9, 1949 (1958).
5. Cobine, James Dillon, "Gaseous Conductors Theory and Engineering Applications", Dover Publications, Inc., New York, 1958.
6. Kushnir, R. M., Palyuhk, B. M., and Sena, L. A., Bull. Ac. Sci., Physical Sci., USSR, 23, 995, (1959).
7. TRW Ion Engine Staff, "Summary Report on Electron Bombardment Ion Engine Development", Final Report on Contract NAS3-2522, TRW ER-5805.

REPORT DISTRIBUTION LIST FOR CONTRACT NO. NAS8-2527

NASA Lewis Research Center (1)
Spacecraft Technology Procurement Section
21000 Brookpark Road
Cleveland, Ohio 44135
Attention: John H. DeFord

NASA Lewis Research Center (1)
Technology Utilization Office
21000 Brookpark Road
Cleveland, Ohio 44135
Attention: John Weber

NASA Marshall Space Flight Center (1)
Huntsville, Alabama
Attention: M-RP-DIR/Dr. E. Stuhlinger

NASA Headquarters (2)
FOB-10B
600 Independence Avenue, Southwest
Washington, D. C. 20546
Attention: RNT/James Lazar

Commander (1)
Aeronautical Systems Division
Wright-Patterson Air Force Base, Ohio
Attention: AFAPL (APIE)/Lt. Robt. Supp

Jet Propulsion Laboratory (1)
4800 Oak Grove Drive
Pasadena, California
Attention: J. J. Paulson

Electro-Optical Systems, Inc. (1)
125 North Vinedo Avenue
Pasadena, California
Attention: R. C. Speiser

General Electric Company (1)
Flight Propulsion Laboratory
Cincinnati, Ohio 45215
Attention: M. L. Bromberg

Ion Physics Corporation (1)
Burlington, Massachusetts
Attention: Dr. S. V. Nablo

Space Technology Laboratories (1)
8433 Fallbrook Avenue
Canoga Park, California
Attention: Dr. D. Langmuir

AFWL (1)
WLPC/Capt. C. F. Ellis
Kirtland Air Force Base
New Mexico

NASA Lewis Research Center (1)
Reports Control Office
21000 Brookpark Road
Cleveland, Ohio 44135

North American Aviation, Inc. (1)
12214 Lakewood Avenue
Downey, California
Attention: Technical Information Office
Department 4096-314

NASA Lewis Research Center (2)
Library
21000 Brookpark Road
Cleveland, Ohio 44135

Aerojet-General (1)
Nucleonics Division
San Ramon, California
Attention: Mr. J. S. Luce

Hughes Research Laboratories (1)
Malibu Canyon Road
Malibu, California
Attention: Dr. G. R. Brewer

NASA Lewis Research Center
Spacecraft Technology Division
21000 Brookpark Road
Cleveland, Ohio 44135
Attention: J. H. Childs (2)
D. L. Lockwood (1)
R. D. Shattuck (1)
J. A. Wolters (7)

United Aircraft Corporation (1)
Research Laboratories
East Hartford 8, Connecticut
Attention: R. J. Meyerand, Jr.

NASA Lewis Research Center
Electromagnetic Propulsion Division
21000 Brookpark Road
Cleveland, Ohio 44135
Attention: W. R. Mickelsen (1)
W. Moeckel (1)

Westinghouse Astronuclear Laboratories (1)
Pittsburgh, Pennsylvania 15234
Attention: Electric Propulsion Lab.
Mr. W. H. Szymanowski

NASA Scientific and Technical Information
Facility (6 + 1 Reproducible Master)
Box 5700
Bethesda, Maryland 20014
Attention: NASA Representative RQT-2448

Aerospace Corporation (1)
P. O. Box 95085
Los Angeles, California 90045
Attention: Library Technical Documents
Group